CHARACTERIZATION OF GENETIC ALTERATIONS IN THE CARDIAC HCN4 CHANNEL

Vom Fachbereich Biologie der Technischen Universität Darmstadt
zur Erlangung des akademischen Grades
eines Doctor rerum naturalium
genehmigte Dissertation von

Dipl.-Biol. Stephanie Biel
aus Pinneberg

1. Referent/Referentin: Prof. Dr. Gerhard Thiel
2. Referent/Referentin: Prof. Dr. Bodo Laube
3. Referent/Referentin: PD Dr. Silke Kauferstein

Tag der Einreichung: 29.05.2015
Tag der mündlichen Prüfung: 16.07.2015
Darmstadt 2015
D17

„Im Herzen eines Menschen
ruht der Anfang und das Ende aller Dinge.“

Leo (Lew) Nikolajewitsch Graf Tolstoi (1828 - 1910),
russischer Erzähler und Romanautor

CONTENTS

CHAPTER 1 – GENETIC SCREENING AND MUTATION ANALYSIS OF THE *HCN4* GENE IN ASSOCIATION WITH BRUGADA AND SICK SINUS SYNDROME

1.1. Abstract

Diseases such as the Sick Sinus and the Brugada Syndrome are based on cardiac abnormalities, which could be caused by a number of genetic aberrances. Over the last years, several mutations have been indentified in genes, which could be associated with both syndromes. *HCN4* is one of these genes; it encodes the hyperpolarization-activated, cyclic nucleotide-gated ion channel 4, which is as pacemaker channel responsible for the autonomic oscillatory function of the sinoatrial node. Mutations in this gene have already been associated with the Sick Sinus and the Brugada Syndrome.

In the present study, we performed a genetic screening of patients with suspected or diagnosed Brugada or Sick Sinus Syndrome to identify new mutations in the *HCN4* gene. This should provide a better understanding of the genetic basis underlying these diseases and their genotype-phenotype correlations.

In one out of 62 samples we found the novel mutation V492F, which is located in the highly conserved pore region of the HCN4 protein. The localization of the mutation in a critical and highly conserved site in the HCN4 channel suggests that the novel mutation V492F may take a significant influence on the functional activity of the cardiac HCN4 channel. This could be the reason for the occurrence of typical symptoms of the diseases in a patient, who is carrying this new discovered sequence alteration.

1.2. Introduction

Sick Sinus Syndrome (SSS) is a general term describing a variety of cardiac arrhythmias, according to the International Classification of Disease-revision 9-Clinical Modification (ICD-9-CM) code 427.81 [1,2]. It is characterized by the symptomatic dysfunction of the sinoatrial node leading to an abnormal cardiac impulse formation and an abnormal electrical propagation from the node to the myocardial tissue [3]. Generally, SSS is a disease of aging occurring predominantly in the elderly, but it can also affect persons of all age and gender [1,3]. Its clinical manifestations are arrhythmias in form of sinus bradycardia, sinus pauses or arrest for a duration longer than 2 or 3 seconds [4], sinoatrial block or alternating bradyarrhythmias and tachyarrhythmias. These can lead to chronotropic incompetence, dizziness, syncopes, palpitations or atrial fibrillation until sudden cardiac arrest [4-6].

The diagnosis of SSS is very difficult, because all these symptoms are phenotypic and may be mild or very intermittent from case to case. Many persons with an early state of SSS show no symptoms as described above and do not feel any signs of illness, whereas those with more advanced disease may present symptoms [1,3,4]. Some extrinsic factors like the wrong use of certain pharmacologic agents can also cause typical symptoms of Sick Sinus Syndrome [3]. Therefore, it is essential to examine carefully all details of current medication and medical history or other diseases before diagnosing a patient with syndromes consistent with SSS [1,4].

Some findings of Sick Sinus Syndrome can be associated with other cardiac abnormalities such as the Brugada Syndrome (BrS) [3,7,8]. BrS was first described by Pedro and Josep Brugada in 1992 [9] as a familial disease with an autosomal dominant inheritance [7,10,11]. This syndrome exhibits rare cardiac arrhythmias with a typical electrocardiographic pattern, as shown in a consensus report endorsed by the European Heart Rhythm Association and the Heart Rhythm Society in 2005 [10,11]. Currently, three electrocardiogram (ECG) abnormalities are recognized in the right precordial leads (V1-3) (figure 1):

Type 1 is characterized by a coved ST-segment elevation of ≥ 2 mm followed by a negative T-wave and Type 2 also by a ST-segment elevation, but followed by a positive or biphasic T-wave that results in a saddle-back configuration. Type 3 shows a right precordial ST-segment elevation of ≤ 1 mm either with coved or saddle-back morphology [10,11].

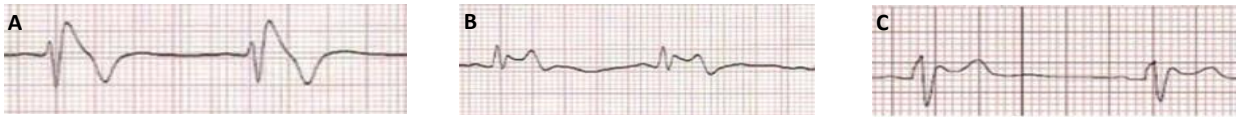

Figure 1: BrS typical ECG abnormalities in the right precordial leads (V1-3).

(A) Type 1 is characterized by a coved ST-segment elevation of ≥ 2 mm followed by a negative T-wave. **(B)** Type 2 is characterized by a ST-segment elevation, but followed by a positive or biphasic T-wave that results in a saddle-back configuration. **(C)** Type 3 shows a right precordial ST-segment elevation of ≤ 1 mm either with coved or saddle-back morphology. Figure modified from Wilde *et al.* 2002 [11].

These electrocardiographic signatures of the syndrome are very dynamic and often concealed, but can be unmasked by a test with potent sodium channel blockers such as flecainide, ajmaline or procainamide [7,11]. Especially, in patients with type 2 or type 3 ECGs, the test is recommended to clarify the diagnosis, because both types occur spontaneously and are not diagnostic of the BrS [7,12]. The diagnosis of Brugada Syndrome is only considered positive if a type 2 or 3 ECG pattern converts to a type 1 ECG pattern with or without provocation by a sodium channel-blocking agent.

The conversion of type 3 to type 2 ST-segment elevation is considered inconclusive for this diagnosis [7,10-12]. Additionally, patients should present at least one of the following criteria: documented ventricular fibrillation, self terminating polymorphic ventricular tachycardia, a family history of sudden cardiac death (<45 years), coved type ECGs in family members, electro-physiological inducibility, syncopes or nocturnal agonal respiration [10,11].

Like SSS, BrS is based on clinical and electrocardiographic features [3]. Therefore, asymptomatic patients with an abnormal ECG only on drug challenge have a benign prognosis [7,10,11]. The appearance of the ECG features without clinical symptoms is referred to an idiopathic Brugada ECG pattern, not Brugada Syndrome. So, before diagnosing BrS it is essential to exclude other factors which may account for those ECG alterations [7,8,11].

Unfortunately, in almost one-third of the patients with Brugada Syndrome, symptoms like syncopes or sudden cardiac death are the only signs of the disease. Moreover, in some cases sudden cardiac death occurs as the first and last symptom, predominantly in young males (8-10 times more than in females) with structurally normal heart and during sleep or rest, particular during the early morning hours [7,9–11,13]. The symptoms usually appear around an age of 45 years, but there are reports of patients affected from 2 days to 84 years [8,10]. However, the majority of patients remain completely asymptomatic, which makes it difficult to estimate the prevalence of the disease. Because of the incomplete penetrance and dynamic ECG manifestations the diagnosis of BrS is complicated [10,12].

Many studies have shown that the Sick Sinus Syndrome may also be a part of BrS and that Brugada typical ECG-types were found in patients with SSS as well [8,9,14]. Therefore, Konstantinos *et al.* [15] and Hiroshi *et al.* [16] investigated the incidence of sinus node dysfunctions (SND) in patients with a Brugada-type ECG. Both came to the same conclusion that SND is not uncommon in these patients and thus, the possibility of SSS should always be taken into consideration in patients with BrS or Brugada-type ECGs. Additionally, Konstantinos *et al.* [15] reported in a further independent study that SSS and BrS may occur simultaneously.

Both diseases could be caused by a number of genetic abnormalities in genes encoding subunits of cardiac sodium, potassium and calcium channels, as well as in genes involved in the trafficking or regulation of these channels [5,10,13]. The gene *SCN5A,* which encodes the α-subunit of the voltage-dependent cardiac sodium channel, was the first gene to be associated with both syndromes, and it still represents the main pathogenic gene in up to 30% of the BrS cases [5,17,18]. But till now, more than 350 pathogenic mutations in several genes have been published, among others in the gene *HCN4* [10,18,19]. *HCN4* encodes the hyperpolarization-activated, cyclic

nucleotide-gated ion channel, which is important for the function of the sinoatrial node and its association with diseases like BrS and SSS increases annually. Over the last years more and more mutations in *HCN4* have been identified in patients with Sick Sinus and Brugada Syndrome [20-22].

In the present study, we performed a genetic screening of patients with suspected or diagnosed Sick Sinus or Brugada Syndrome to identify new mutations in the *HCN4* gene and thereby, to get a better understanding about the genetic underlying of these diseases and their genotype-phenotype correlations.

1.3. Material and Methods

For the genetic screening of the *HCN4* gene, 62 blood samples were extracted with phenol-chloroform to isolate the genomic DNA. The majority of the samples was from patients with a suspected diagnosis of Sick Sinus or Brugada Syndrome (n=37) and two smaller sections were from clinically confirmed patients with Sick Sinus (n=11) and Brugada Syndrome (n=14), respectively (figure 2). The whole coding regions and the exon-intron-boundaries of the *HCN4* gene were amplified by polymerase chain reaction (PCR) with primers designed by Schulze-Bahr *et al.*, 2003 [22] (see appendix, table 2). The PCR-products were examined by agarose gel electrophoresis and direct sequencing was performed on an ABI 3130 genetic analyzer, Applied Biosystems. The data analysis occurs with the program SeqScape V2.5 and the NCBI-reference sequence (National Center of Biotechnology) NG_009063.1.

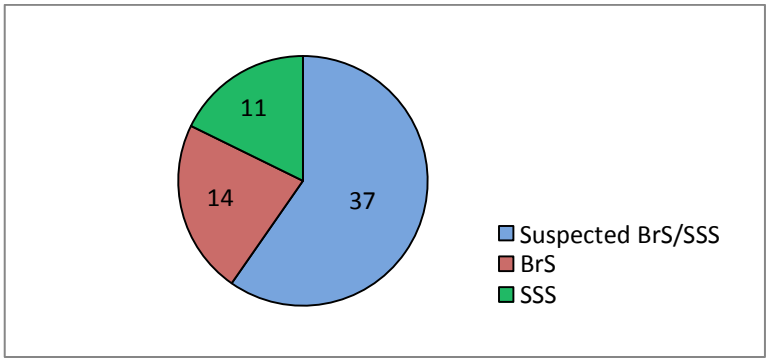

Figure 2: Allocation of the examined blood samples (n=62; Suspected BrS/SSS=37, BrS=14; SSS=11).

1.4. Results

1.4.1. *HCN4* Sequencing

By sequencing the *HCN4* gene in samples of 62 patients with suspected or diagnosed Sick Sinus or Brugada Syndrome, we detected seven sequence variations, which are shown in table 1.

Table 1: Overview of all detected sequence variations in the *HCN4* gene.

exon	base exchange	AA exchange	AA position	protein region
1	CTC → CTG	Leu (L) → Leu (L)	L12L	N-terminus
1	GGG → GAG	Gly (G) → Glu (E)	G36E	N-terminus
4	GTC → TTC	Val (V) → Phe (F)	V492F	pore region
4	CTG → TTG	Leu (L) → Leu (L)	L520L	C-terminus
8	CAC → CAT	His (H) → His (H)	H727H	C-terminus
8	CCG → CCA	Pro (P) → Pro (P)	P852P	C-terminus
8	CCA → CCG	Pro (P) → Pro (P)	P1200P	C-terminus

Figure 3 illustrates the positions of these variants within the HCN4 protein. The sequence alterations L12L and G36E are located at the beginning of the N-terminus, V492F in the pore region and L520L, H727H, P852P, P1200P in the area of the C-terminal loop.

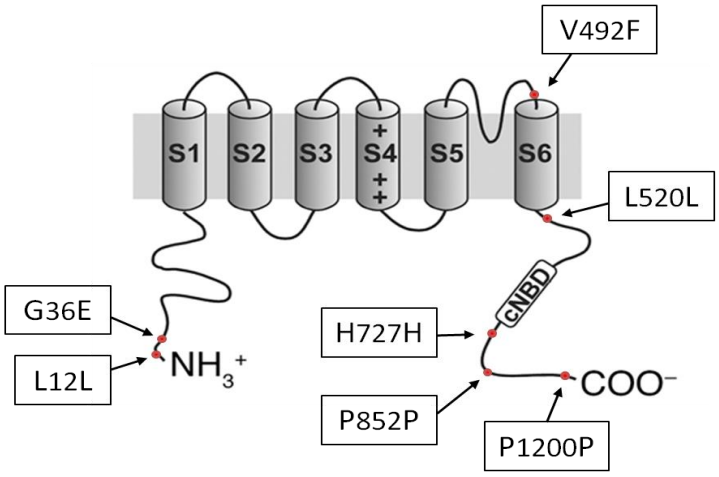

Figure 3: Positions of alterations identified within the HCN4 protein.

Modified from Schulze-Bahr *et al.*, 2003 [22].

1.4.2. Sequence variant L12L

The sequence alteration L12L is located in exon 1 of the *HCN4* gene. The heterozygous base exchange from cytosine to guanine (CT**C** → CT**G**) on the third position of the coding triplet causes no replacement of the primary amino acid. The amino acid leucine is preserved at the protein position 12. Databases like that of the National Center for Biotechnology Information (NCBI) classify this aberrance as a non-pathogenic variant with a frequency of 0.36%.

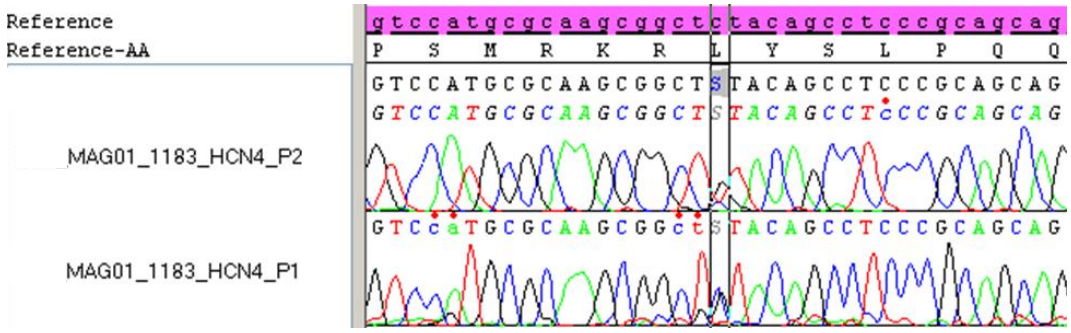

Figure 4: Part of the electropherogram of the sample MAG01-1183.
A heterozygous sequence variant L12L is shown in exon 1, visible by the overlapping bases of cytosine by guanine in the marked area. Degenerated code: S = C+G. P1 = forward primer; P2 = reverse primer; AA = amino acid.

1.4.3. Sequence variant G36E

Also in exon 1 located is the alteration G36E. This sequence variation is due to a heterozygous base exchange from guanine to adenine (G**G**G → G**A**G) in the second position of the coding triplet leading to an amino acid substitution. At the protein position 36 the amino acid glycine is substituted by glutamic acid. According to the NCBI database, this variant appears in 2.5% of the population and up to now no pathological consequences have been reported in the literature. The substitution G36E is located in a not highly conserved region of the protein and, therefore, considered as a sequence variant with no functional modification.

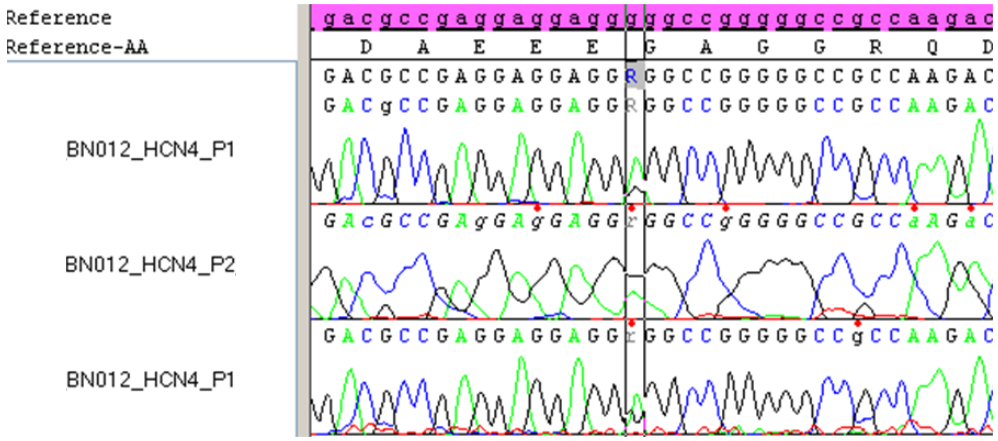

Figure 5: Part of the electropherogram of the sample BN012.

A heterozygous sequence variant G36E is shown in exon 1, visible by the overlapping bases of guanine by adenine in the marked area. Degenerated code: R = G+A. P1 = forward primer; P2 = reverse primer; AA = amino acid.

1.4.4. Sequence variant L520L

In 11% of the blood samples, the already known sequence alteration L520L was detected in exon 4 of the *HCN4* gene. It is a heterozygous base exchange from cytosine to thymine (**C**TG → **T**TG) on the first triplet position. The resulting amino acid at protein position 520 remains unchanged, because both triplet variants encode leucine. This sequence variation is present in 5.31% of the population and listed in the NCBI database.

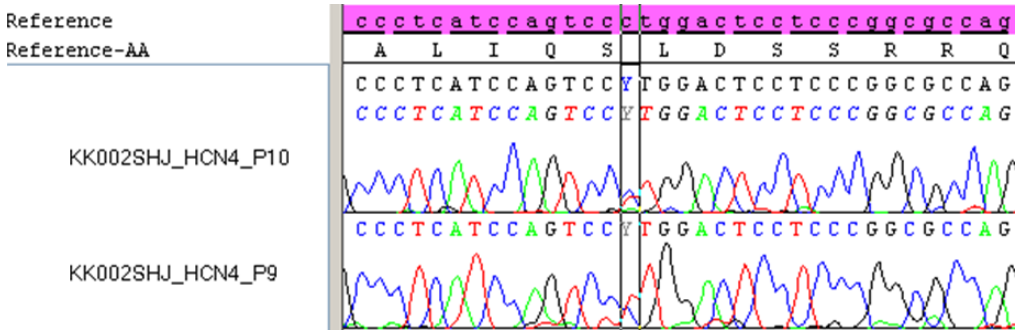

Figure 6: Part of the electropherogram of the sample KK002SHJ.

A heterozygous sequence variant L520L is shown in exon 4, visible by the overlapping bases of cytosine by thymine in the marked area. Degenerated code: Y = C+T. P9 = forward primer; P10 = reverse primer; AA = amino acid.

1.4.5. Sequence variant H727H

The variation H727H was found in exon 8 of the *HCN4* gene and is already registered in the NCBI database as a sequence variation with a frequency of 0.04% in the population. This heterozygous base exchange from cytosine to thymine (CA**C** → CA**T**) on the third position of the coding triplet is not leading to an amino acid exchange at the position 727 of the protein.

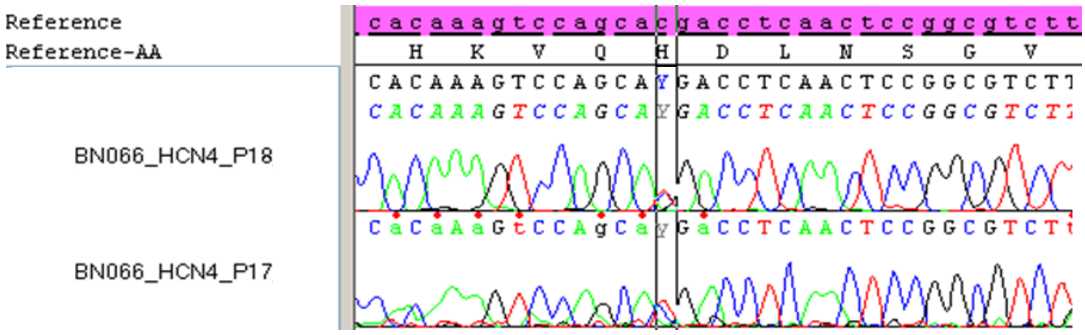

Figure 7: Part of the electropherogram of the sample BN066.

A heterozygous sequence variant H727H is shown in exon 8, visible by the overlapping bases of cytosine by thymine in the marked area. Degenerated code: Y = C+T. P17 = forward primer; P18 = reverse primer; AA = amino acid.

1.4.6. Sequence variant P852P

The heterozygous base exchange from guanine to adenine (CC**G** → CC**A**) on the third triplet position causes no amino acid replacement of proline at the position 852 in the HCN4 protein. This sequence variation is located in exon 8 of the gene and listed in the NCBI database as a non-pathogenic variant with a prevalence of 2.76% in the population.

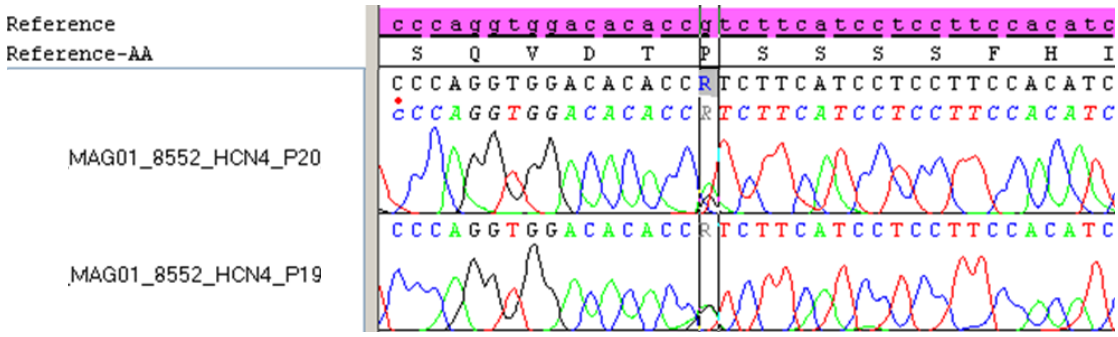

Figure 8: Part of the electropherogram of the sample MAG01-8552.

A heterozygous sequence variant P852P is shown in exon 8, visible by the overlapping bases of guanine by adenine in the marked area. Degenerated code: R = G+A. P19 = forward primer; P20 = reverse primer; AA = amino acid.

1.4.7. Sequence variant P1200P

The sequence alteration P1200P is also located in exon 8 of the *HCN4* gene and was found in each sample of this study. The both heterozygous as well as homozygous base exchange from adenine to guanine (CC**A** → CC**G**) on the third triplet position represents a non-pathogenic sequence variation, where the amino acid proline in position 1200 of the HCN4 protein is not replaced. P1200P is already listed in the NCBI database with a frequency of 14.04%.

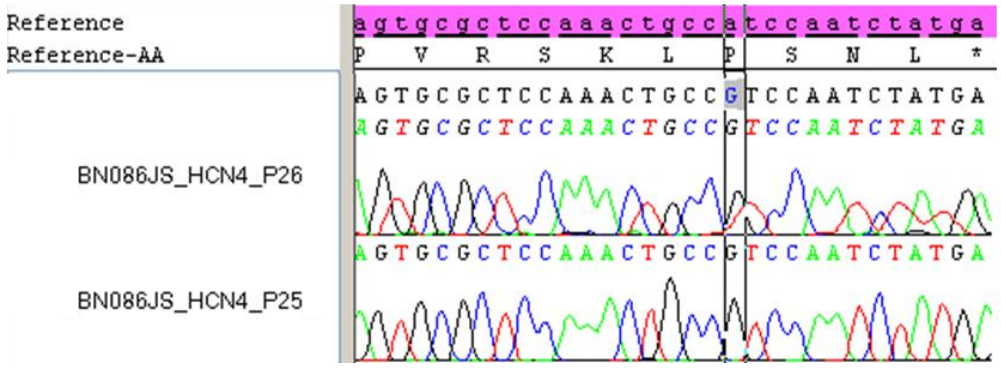

Figure 9: Part of the electropherogram of the sample BN086JS.

A homozygous sequence variant P1200P is shown in exon 8, visible by the aberrant base guanine of the reference sequence in the marked area. P25 = forward primer; P26 = reverse primer; AA = amino acid.

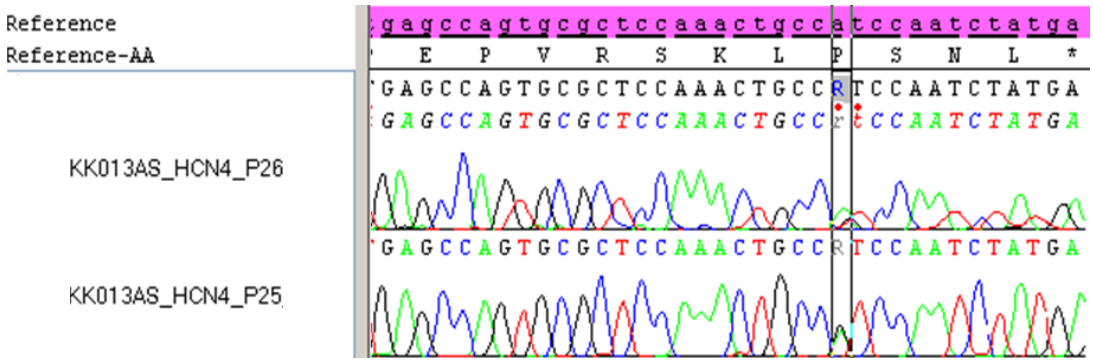

Figure 10: Part of the electropherogram of the sample KK013AS.

A heterozygous sequence variant P1200P is shown in exon 8, visible by the overlapping bases of adenine by guanine in the marked area. Degenerated code: R = G+A. P25 = forward primer; P26 = reverse primer; AA = amino acid.

1.4.8. Sequence variant V492F

This heterozygous base exchange from guanine to thymine (**G**TC → **T**TC) on the first position of the coding triplet is a new alteration in exon 4 of the *HCN4* gene, which is leading to an amino acid replacement of valine by phenylalanine at the protein position 492.

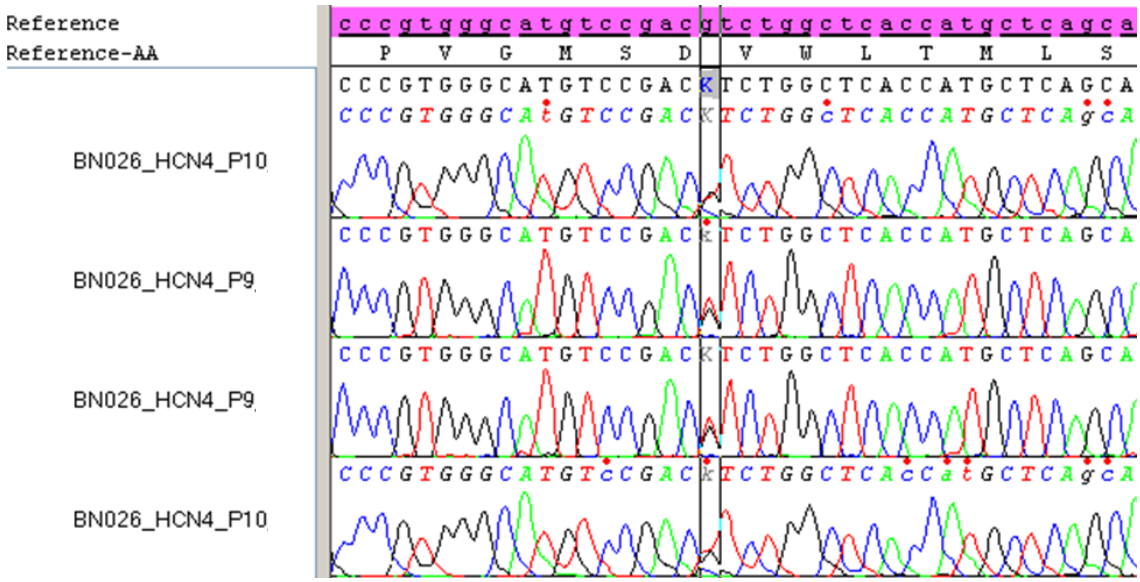

Figure 11: Part of the electropherogram of the sample BN026.

The heterozygous sequence variant V492F is shown in exon 4, visible by the overlapping bases of guanine by thymine in the marked area. Degenerated code: K = G+T. P9 = forward primer; P10 = reverse primer; AA = amino acid.

Since this sequence variation has not been listed in the databases, 100 samples from healthy persons were screened to verify whether it is a common polymorphism or a mutation. This variant was not detected in any of these samples and is consequently considered to be a mutation.

The location of V492F is determined in the highly conserved pore region of the HCN4 channel (figure 12). According to some already known mutations in this area (G480R [21], Y481H [23], G482R [24] or A485V [25]), this variant seems to have a significant influence on the functional activity of the cardiac HCN4 channel. Because all these sequence alterations mentioned are leading to a reduced channel conductance resulting in sinus bradycardia.

human	...GYGRQAPVGMSDVWLTMLSMIVGATCYAMFIGH...
mouse	...GYGRQAPVGMSDVWLTMLSMIVGATCYAMFIGH...
rat	...GYGRQAPVGMSDVWLTMLSMIVGATCYAMFIGH...
whale	...GYGRQAPMGMSDVWLTMLSMIVGATCYAMFIGH...
cattle	...GYGQQAPVGMSDVWLTMLSMIVGATCYAMFIGH...
mole	...GYGQQAPVGMSDVWLTMLSMIVGATCYAMFIGH...
hamster	...GYGQQAPVGMSDVWLTMLSMIVGATCYAMFIGH...

Figure 12: Protein sequences of the highly conserved HCN4 pore region from different individuals.

An additional evaluation of this new sequence variation V492F by using the PolyPhen-2 software predicted a very probable pathogenicity as well (figure 13). PolyPhen-2 (Polymorphism Phenotyping v2) is a software tool which predicts possible impact of an amino acid substitution on the structure and function of human proteins using straightforward physical and evolutionary comparative considerations (genetics.bwh.harvard.edu/pph2/).

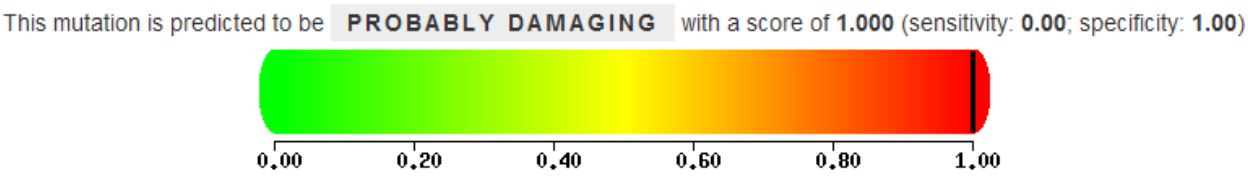

Figure 13: Evaluation of the new HCN4-V492F mutation by PolyPhen-2.

Mutation is predicted to be probably damaging with a score of 1.000. The PolyPhen-2 score represent the probability that a substitution is damaging. Values near 1 are more confidently predicted to be deleterious.

1.4.9. Percentage distribution of all alterations

Figure 14 shows the percentage distribution of all sequence variations in all samples (n=62). As can be seen, the most alterations occur in relatively low percentage in contrast to the polymorphism P1200P, which was found in 100% of the samples. It is also the only variant that occurred both in hetero- and homozygous traits. In the majority of the cases it was found as a homozygous aberrance (85%) and only 15% were heterozygous. The other alterations were only present in heterozygous traits and in a lower distribution.

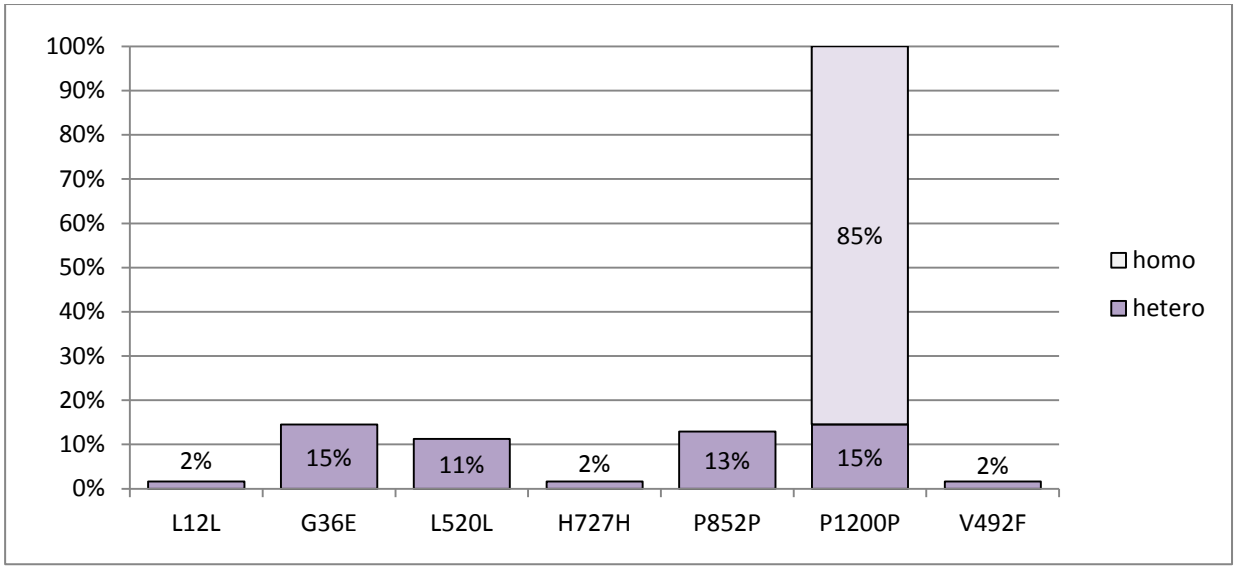

Figure 14: Percentage distribution of the sequence variations detected (see table 2) in all samples (n=62).

Figures 15 and 16 present the percentage distribution of all variants in the various patient groups. In figure 15 the alterations P1200P was omitted (and exposed in figure 16), because it is the only variant in this study which occurred both in heterozygous and homozygous traits, whereas all others were heterozygous. Figure 15 shows that the sequence variant L12L was only present in one patient of the BrS samples, while H727H and V492F were only detected in one patient with suspected BrS or SSS diagnosis, respectively. The aberrances G36E (n=9), L520L (n=7) and P852P (n=8) were found in all three patient groups.

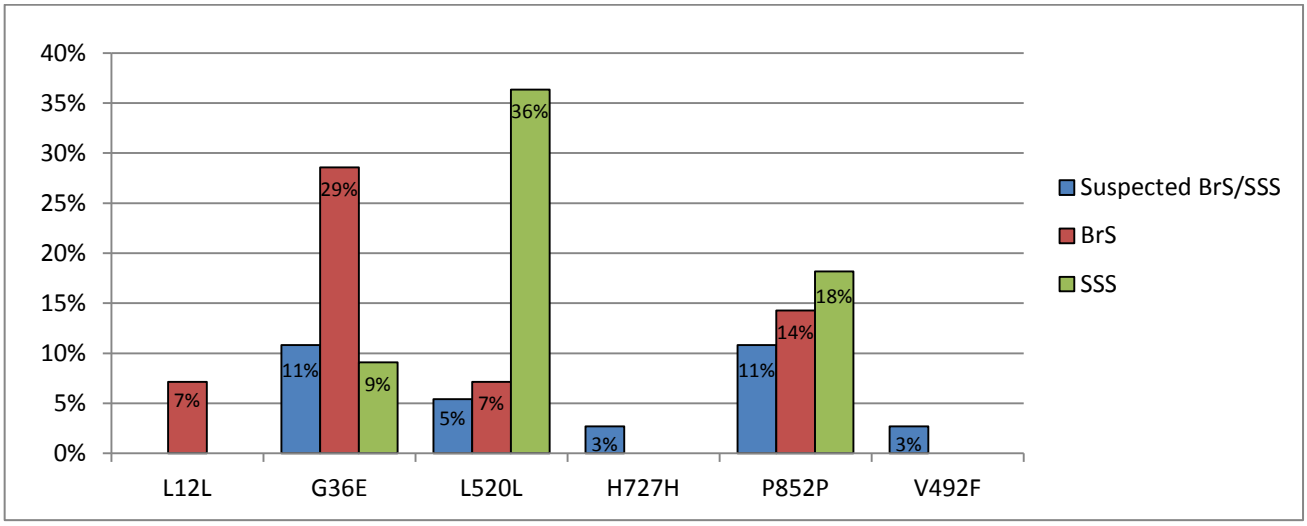

Figure 15: Percentage distribution of heterozygous sequence variations of *HCN4* in the three patient groups.

Figure 16 displays the homo-hetero arrangement of the sequence variation P1200P among the three patient groups. Homozygosity was found only in the SSS samples, whereas both traits (homo- and heterozygous) were present in patients with BrS and suspected BrS or SSS, respectively.

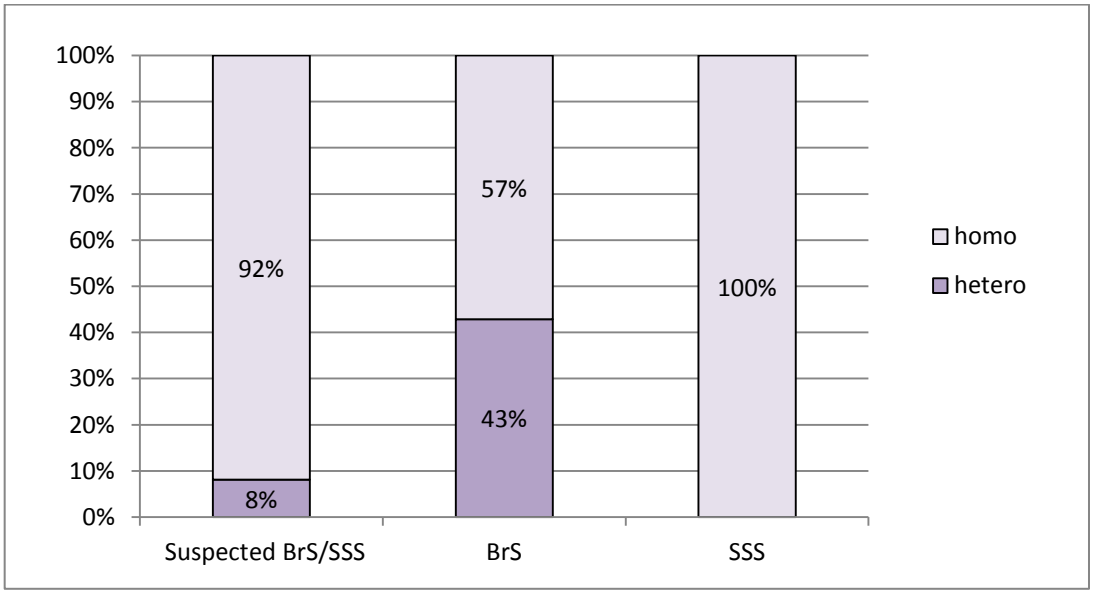

Figure 16: Homo-hetero arrangement of the HCN4 sequence variation P1200P among the three patient groups.

1.5. Discussion

Sick Sinus and Brugada Syndrome are both diseases with a strong genetic basis. Several mutations have been identified in genes encoding subunits of cardiac sodium, potassium and calcium channels, which may be associated with SSS or BrS [10,26]. Over the last years, especially the genetics of BrS was found to be complex. In addition to *SCN5A* mutations, others were identified in more than 17 genes [18,27]. The knowledge about BrS associated mutations is rapidly increasing, pointing to the importance of genetic screening in view of the diagnosis or treatment [18]. *HCN4* is one of the genes, which are important for the uninterrupted function of the sinoatrial node and, therefore, may play an essential part in both diseases.

For a better understanding of the role of *HCN4* in these diseases, 62 patients with suspected or diagnosed SSS or BrS were genetically screened to identify novel mutations in the *HCN4* gene. In the coding region of *HCN4* we found six already known and one novel sequence alteration, V492F. Of all these variants, two are located in exon 1 (N-terminus), two in exon 4 (one in the pore and one in the beginning of the C-terminus loop) and three in exon 8 (C-terminus loop). Except G36E and the new V492F, all base exchanges detected are not resulting in a substitution of the primary amino acid. Through the exchange of guanine by adenine in exon 1, glycine was substituted by glutamine acid at the protein position 36, which is located in a not highly conserved region. However, G36E and all other aberrances without an amino acid replacement are listed in the NCBI database as sequence variations without functional modification of the channel activity. Since V492F was not listed in the database, 100 samples of healthy persons were screened to clarify whether it is a common polymorphism or a mutation. This variation was not found in any of these samples and, therefore, it should be considered as a novel mutation.

Regarding the percentage distribution of the sequence aberrances, it is evident that one of the variants, P1200P, appears in each sample, although the NCBI database report a incidence of just 14.04% in the population. It is the only variant, which occurs both in heterozygous and homozygous traits. In the three patient groups, the homozygous form of P1200P was predominantly found in patients with the diagnosis of Sick Sinus Syndrome (100%) as well as in patients with suspected SSS or BrS (92%). But also in the group of patients with a clear diagnosis of BrS, more than half of the cases (57%) exhibited the homozygous variant. Thus, it seems that the most common form of P1200P is the homozygous variant, whereas the other sequence alterations occur only in heterozygous traits.

The novel mutation V492F was detected in only one of the cases. This case was a young male, 18 years old, with a presumed Brugada Syndrome diagnosis. He was suffering from dizziness and

multiple syncopes in situations of rest. Cardiological investigations like echocardiography and MRT revealed no morphological abnormalities such as myocarditis or arrhythmogenic right ventricular cardiomyopathy. But the long term ECG displayed tachycardia and ST segment elevation in the right precordial leads, which is followed by a positive T-wave (Brugada-type 2, see figure 1). By testing with ajmaline, the diagnostic findings were confirmed and a Brugada Syndrome could not be excluded. In this case the results of the genetic screening of the *HCN4* gene support the diagnosis of BrS, because the novel mutation is located in the highly conserved pore region of the hyperpolarisation-activated cyclic nucleotide-gated channel 4, which is a pacemaker channel responsible for the autonomic function of the sinoatrial node. Mutations in this gene have already been associated with sinus node dysfunctions and the Brugada Syndrome [28,29].

The fact that V492F is located in the highly conserved pore region of the channel and the prediction of the subsequent analysis by using the PolyPhen-2 software, which is based on a number of features comprising the sequence, phylogenetic and structural information characterizing the substitution suggests a potential damaging effect. The examination of already known mutations in this area (G480R [21], Y481H [23], G482R [24] or A485V [25]) has shown that an amino acid exchange within the conserved pore region is leading to a reduced conductance of the channel resulting in sinus bradycardia. So, the sequence variation V492F may also have a significant influence on the functional activity of the cardiac HCN4 channel. Through the base exchange of guanine by thymine on the first position of the coding triplet, the primary amino acid valine is replaced by phenylalanine at the protein position 492. Both amino acids have the same physical properties, but phenylalanine has a bigger volume and is also more than double heavier than valine. This may be the reason for a functional modification of the activity and gating of the channel and, therefore, for the clinical and electrocardiographic features in this case. However, for a definite assessment of the influence of this novel mutation V492F, further electrophysiological examinations are needed (see chapter 2). At this time, the physicians gave the patient advice for an implantable cardioverter defibrillator (ICD).

Because of the autosomal dominant inheritance of the Brugada Syndrome, it is recommended to screen first-degree relatives for causal mutations and/or probably present clinical symptoms [7,8]. The identification of BrS mutation carriers may be used to trace undiagnosed and/or asymptomatic patients at a potential risk [7,30]. In the present case, the parents of the young male were asymptomatic and their electrocardiogram showed no pathologic alterations. Thus, they declined the genetic testing.

In summary, in cases of suspected Brugada or Sick Sinus Syndrome, such a genetic testing, which may support the clinical diagnosis, is highly recommended and may reveal an early identification of

relatives at potential risk. It will also contribute to the understanding of the underlying genetics and their genotype-phenotype relationship of these diseases [7,18,30].

1.6. References

[1] G.A. Ewy, Sick Sinus Syndrome, Journal of the American College of Cardiology 64 (2014) 539–540.

[2] P.N. Jensen, N.N. Gronroos, L.Y. Chen, A.R. Folsom, C. deFilippi, S.R. Heckbert, A. Alonso, Incidence of and Risk Factors for Sick Sinus Syndrome in the General Population, Journal of the American College of Cardiology 64 (2014) 531–538.

[3] M. Semelka, J. Gera, S. Usman, Sick sinus syndrome: a review, Am Fam Physician 87 (2013) 691–696.

[4] G. Gregoratos, Sick Sinus Syndrome, Circulation 108 (2003) 143e–144.

[5] J.B. Anderson, D.W. Benson, Genetics of Sick Sinus Syndrome, Cardiac Electrophysiology Clinics 2 (2010) 499–507.

[6] K.B. Keller, L. Lemberg, The sick sinus syndrome, Am. J. Crit. Care 15 (2006) 226–229.

[7] C. Antzelevitch, Brugada Syndrome: Report of the Second Consensus Conference: Endorsed by the Heart Rhythm Society and the European Heart Rhythm Association, Circulation 111 (2005) 659–670.

[8] E. Arbelo, J. Brugada, Risk Stratification and Treatment of Brugada Syndrome, Curr Cardiol Rep 16 (2014).

[9] P. Brugada, J. Brugada, Right bundle branch block, persistent ST segment elevation and sudden cardiac death: A distinct clinical and electrocardiographic syndrome, Journal of the American College of Cardiology 20 (1992) 1391–1396.

[10] R. Brugada, O. Campuzano, G. Sarquella-Brugada, J. Brugada, P. Brugada, Brugada syndrome, Methodist Debakey Cardiovasc J 10 (2014) 25–28.

[11] A.A. Wilde, Proposed Diagnostic Criteria for the Brugada Syndrome: Consensus Report, Circulation 106 (2002) 2514–2519.

[12] J. Jellins, M. Milanovic, D.-J. Taitz, S.H. Wan, P.W. Yam, Brugada syndrome, Hong Kong Med J 19 (2013) 159–167.

[13] A.S. Sheikh, K. Ranjan, Brugada syndrome: a review of the literature, Clin Med 14 (2014) 482–489.

[14] H. Hayashi, M. Sumiyoshi, M. Yasuda, K. Komatsu, G. Sekita, Y. Kawano, T. Tokano, Y. Nakazato, H. Daida, Prevalence of the Brugada-Type Electrocardiogram and Incidence of Brugada Syndrome in Patients With Sick Sinus Syndrome, Circ J 74 (2010) 271–277.

[15] K.P. Letsas, P. Korantzopoulos, M. Efremidis, R. Weber, L. Lioni, G. Bakosis, V.P. Vassilikos, S. Deftereos, A. Sideris, T. Arentz, Sinus node disease in subjects with type 1 ECG pattern of Brugada syndrome, Journal of Cardiology 61 (2013) 227–231.

[16] H. Morita, K. Fukushima-Kusano, S. Nagase, K. Miyaji, S. Hiramatsu, K. Banba, N. Nishii, A. Watanabe, M. Kakishita, S. Takenaka-Morita, K. Nakamura, H. Saito, T. Emori, T. Ohe, Sinus node function in patients with Brugada-type ECG, Circ. J. 68 (2004) 473–476.

[17] M.J. Ackerman, S.G. Priori, S. Willems, C. Berul, R. Brugada, H. Calkins, A.J. Camm, P.T. Ellinor, M. Gollob, R. Hamilton, R.E. Hershberger, D.P. Judge, H. Le Marec, W.J. McKenna, E. Schulze-Bahr, C. Semsarian, J.A. Towbin, H. Watkins, A. Wilde, C. Wolpert, D.P. Zipes, HRS/EHRA Expert Consensus Statement on the State of Genetic Testing for the Channelopathies and Cardiomyopathies: This document was developed as a partnership between the Heart Rhythm Society (HRS) and the European Heart Rhythm Association (EHRA), Europace 13 (2011) 1077–1109.

[18] M.W. Nielsen, A.G. Holst, S.-P. Olesen, M.S. Olesen, The genetic component of Brugada syndrome, Front. Physiol. 4 (2013).

[19] K. Ueda, Y. Hirano, Y. Higashiuesato, Y. Aizawa, T. Hayashi, N. Inagaki, T. Tana, Y. Ohya, S. Takishita, H. Muratani, M. Hiraoka, A. Kimura, Role of HCN4 channel in preventing ventricular arrhythmia, J Hum Genet 54 (2009) 115–121.

[20] J.A. Towbin, Ion Channel Dysfunction Associated With Arrhythmia, Ventricular Noncompaction, and Mitral Valve Prolapse, Journal of the American College of Cardiology 64 (2014) 768–771.

[21] E. Nof, D. Luria, D. Brass, D. Marek, H. Lahat, H. Reznik-Wolf, E. Pras, N. Dascal, M. Eldar, M. Glikson, Point Mutation in the HCN4 Cardiac Ion Channel Pore Affecting Synthesis, Trafficking, and Functional Expression Is Associated With Familial Asymptomatic Sinus Bradycardia, Circulation 116 (2007) 463–470.

[22] E. Schulze-Bahr, A. Neu, P. Friederich, U.B. Kaupp, G. Breithardt, O. Pongs, D. Isbrandt, Pacemaker channel dysfunction in a patient with sinus node disease, J. Clin. Invest. 111 (2003) 1537–1545.

[23] A. Milano, A.M. Vermeer, E.M. Lodder, J. Barc, A.O. Verkerk, A.V. Postma, I.A. van der Bilt, M.J. Baars, P.L. van Haelst, K. Caliskan, Y.M. Hoedemaekers, S. Le Scouarnec, R. Redon, Y.M. Pinto, I. Christiaans, A.A. Wilde, C.R. Bezzina, HCN4 Mutations in Multiple Families With Bradycardia and Left Ventricular Noncompaction Cardiomyopathy, Journal of the American College of Cardiology 64 (2014) 745–756.

[24] P.A. Schweizer, J. Schröter, S. Greiner, J. Haas, P. Yampolsky, D. Mereles, S.J. Buss, C. Seyler, C. Bruehl, A. Draguhn, M. Koenen, B. Meder, H.A. Katus, D. Thomas, The Symptom Complex of Familial Sinus Node Dysfunction and Myocardial Noncompaction Is Associated With Mutations in the HCN4 Channel, Journal of the American College of Cardiology 64 (2014) 757–767.

[25] A. Laish-Farkash, M. Glikson, D. Brass, D. Marek-Yagel, E. Pras, N. Dascal, C. Antzelevitch, E. Nof, H. Reznik, M. Eldar, D. Luria, A Novel Mutation in the HCN4 Gene Causes Symptomatic Sinus Bradycardia in Moroccan Jews, Journal of Cardiovascular Electrophysiology 21 (2010) 1365–1372.

[26] G. Lippi, M. Montagnana, T. Meschi, I. Comelli, G. Cervellin, Genetic and clinical aspects of Brugada syndrome: an update, Adv Clin Chem 56 (2012) 197–208.

[27] G. Veerakul, K. Nademanee, Brugada Syndrome, Circ J 76 (2012) 2713–2722.

[28] L. Crotti, C.A. Marcou, D.J. Tester, S. Castelletti, J.R. Giudicessi, M. Torchio, A. Medeiros-Domingo, S. Simone, M.L. Will, F. Dagradi, P.J. Schwartz, M.J. Ackerman, Spectrum and Prevalence of Mutations Involving BrS1- Through BrS12-Susceptibility Genes in a Cohort of Unrelated Patients Referred for Brugada Syndrome Genetic Testing, Journal of the American College of Cardiology 60 (2012) 1410–1418.

[29] K. Ueda, K. Nakamura, T. Hayashi, N. Inagaki, M. Takahashi, T. Arimura, H. Morita, Y. Higashiuesato, Y. Hirano, M. Yasunami, S. Takishita, A. Yamashina, T. Ohe, M. Sunamori, M. Hiraoka, A. Kimura, Functional Characterization of a Trafficking-defective HCN4 Mutation, D553N, Associated with Cardiac Arrhythmia, Journal of Biological Chemistry 279 (2004) 27194–27198.

[30] P.L. Hedley, P. Jörgensen, S. Schlamowitz, J. Moolman-Smook, J.K. Kanters, V.A. Corfield, M. Christiansen, The genetic basis of Brugada syndrome: A mutation update, Hum. Mutat. 30 (2009) 1256–1266.

1.7. Appendix

1.7.1. *HCN4* primer

The used *HCN4* primers were successfully established from literature (Schulze-Bahr *et al.*, 2003 [22]) and the PCR conditions partial modified by a GC KIT (AmpliTaq Gold® 360 DNA Polymerase Kit (1000U), Applied Biosystems) or dimethyl sulfoxide (DMSO).

Table 2: PCR conditions of the used *HCN4* primers. Modified from Schulze-Bahr *et al.*, 2003 [22].

Exon	*HCN4* Primer	Primer Sequence (5´→ 3´)	Fragment Size (bp)	Annealing Temperature	Add on
1	1 2	GCGGCGCCGCGCTCCTGCCC CGCTCGGGCTCGGCCGCCAG	512	65 °C	5% DMSO
1	3 4	CGGCAGCAGTCACGGACACCTGC GGAAAGTTAACTCCGGCTGGGAGGC	533	65 °C	5% DMSO
2	5 6	TCTCTCTTCCTGGCGACTGACCC GGTCAAGAACTTACTAGTATTTGTCC	615	62 °C	
3	7 8	GAGCAGTGCCCACCAGCAGCTC GCCACCCTACCTCTGGAGAGC	322	65 °C	
4	9 10	AGGTTGAGGTGAGTAGGTGGCAGG CTGAAACTCAGATTCTCATCTCAGAGG	489	62 °C	
5	11 12	AGATCTCAAGGAACCAAGTTTAGCC AGGGTGGATTGGGACACGGGAAGG	375	62 °C	
6	13 14	CCTTCCCGTGTCCCAATCCACCCT CCCTACCCTGGGCTCACAGACACC	411	65 °C	
7	15.1 16.1	CCATTTGGTGGGGAAGAGGCATCC ATCAGGTGCAGACCTGGCTTAGGC	277	65 °C	
8	17 18	CCCGCTCTGCCCTGAGTGCCTGT CCGAGGTTGCCCAGCCCAGATCC	310	65 °C	
8	19 20	ACTTCTGTGGCCATAGCCCTCAC GTCGGAGGAGGACAGGGAGCCACC	402	65 °C	
8	21 22	TCCCACACCATCAGCTGGCGTAGC TGCCACAAGGGACGGCGGCTCAGG	369	65 °C	
8	23.1 24.1	CGGGGAGTTGTCCCTAGGTCTGG CTGGGGAAGAGCGGGAAGGCAGC	370	65 °C	GC Kit
8	25 26	CTCAGGACGGGGCGCAGACTCTC GAGAGAAAAGAAGAAAGAAGAGGGAAG	371	62 °C	

1.7.2. Amino acids

A	Ala	Alanine
C	Cys	Cysteine
D	Asp	Asparatic acid
E	Glu	Glutaminic acid
F	Phe	Phenylalanine
G	Gly	Glycine
H	His	Histidine
I	Ile	Isoleucine
K	Lys	Lysine
L	Leu	Leucine
M	Met	Methionine
N	Asn	Asparagine
P	Pro	Proline
Q	Gln	Glutamine
R	Arg	Arginine
S	Ser	Serine
T	Thr	Threonine
V	Val	Valine
W	Trp	Tryptophan
Y	Tyr	Tyrosine

CHAPTER 2 – FUNCTIONAL CHARACTERISTIC OF A NOVEL *HCN4* MUTATION IN A PATIENT WITH BRUGADA SYNDROME

2.1. Abstract

In a previous study we detected a new *HCN4* mutation in a patient with a diagnosed Brugada Syndrome. This new sequence alteration is located in a highly conserved position close to the pore of the HCN4 protein, a channel which is important for a regular impulse generation in the heart.
According to the location of the mutation in a critical domain of the HCN4 channel, which hosts also other functionally relevant mutations, we anticipate that this sequence alteration has an influence on channel function.
We performed electrophysiological investigations in HEK293 cells to study the influence of the new HCN4-V492F pore mutation and of three additional variants of the same protein position, respectively. The recordings of a reduced channel conduction in HEK293 cells expressing the respective mutated channel in comparison to HEK293 cells expressing the HCN4 wildtype showed in all four variants (V492F/-A/-D/-R) the same intensity. Also testing HEK293 cells, which where transfected with DNA of HCN4-WT as well as DNA of HCN4-V492F (1:1), demonstrated a clear reduction of the activation currents.

2.2. Introduction

Cardiac arrhythmias in Brugada Syndrome were found to be caused by genetic abnormalities in the hyperpolarization-activated, cyclic nucleotide-gated channels (HCN) [1], which belong to the family of voltage-gated ion channels. They comprise four isoforms (HCN1-4), which are expressed in the nervous system and the heart. The predominant transcript in the human heart is the isoform HCN4, which is highly expressed in the sinoatrial node [2]. This area of the heart is responsible for the autonomic activity by generating a pacemaker impulse, which in turn produces a regular heart contraction [3]. HCN4 channels are activated by membrane hyperpolarization and exhibit an inward permeation of Na^+ and K^+ ions in a ratio of 1:3 to 1:5 (P_{Na} : P_K) [2].
The HCN4 channel consists of four subunits and each subunit has six transmembrane domains and a cyclic nucleotide-binding domain (CNBD) at the cytosolic COOH terminus [3]. Mutations in the gene encoding the HCN4 channel lead to cardiac dysfunctions, which were found in diseases like the Sick Sinus and Brugada Syndrome [4]. To date, more than 23 mutations in the *HCN4* gene have been identified and associated with clinically established or potential sinus node dysfunctions [5].

In a previous study we detected a new *HCN4* mutation in a patient with a diagnosed Brugada Syndrome (chapter 1). In this case the patient underwent a genetic screening to confirm his clinical manifestations. The results of that screening and an evaluation in advance of this new sequence variation V492F by using the PolyPhen-2 software predicted a potential pathogenicity. V492F is located in the highly conserved pore region of the cardiac pacemaker channel (figure 17 and 18) and because of such a location in a functionally critical position, it can be anticipated that the mutation may affect the channel activity. It was already shown for mutations in several other positions, i.e. G480R [6], Y481H [7], G482R [8] and A485V [9] that they affect the HCN gating.

To test the influence of the new HCN4-V492F mutation, we expressed the mutant channel in HEK293 cells and analyzed the channel by patch-clamp recordings.

human	...GYGRQAPVGMSDVWLTMLSMIVGATCYAMFIGH...
mouse	...GYGRQAPVGMSDVWLTMLSMIVGATCYAMFIGH...
rat	...GYGRQAPVGMSDVWLTMLSMIVGATCYAMFIGH...
whale	...GYGRQAPMGMSDVWLTMLSMIVGATCYAMFIGH...
cattle	...GYGQQAPVGMSDVWLTMLSMIVGATCYAMFIGH...
mole	...GYGQQAPVGMSDVWLTMLSMIVGATCYAMFIGH...
hamster	...GYGQQAPVGMSDVWLTMLSMIVGATCYAMFIGH...

Figure 17: Protein sequences of the highly conserved HCN4 pore region from different vertebrates.

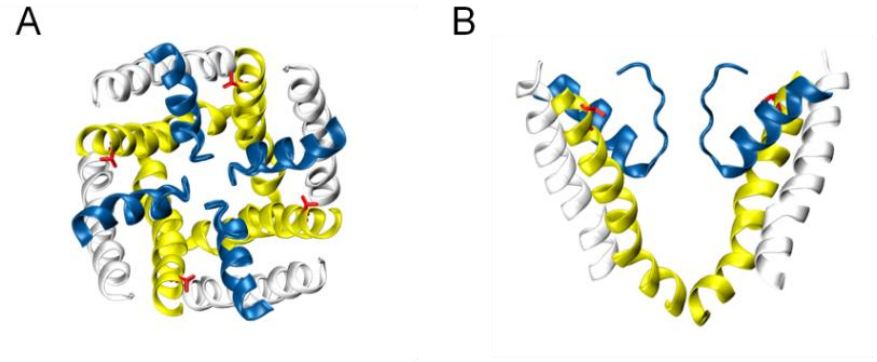

Figure 18: 3D simulation of the HCN4 pore including the novel mutation V492F (red).
(A) Top view and **(B)** side view of the HCN4 pore region. Transmembrane domain S5 (white), pore helix (blue) and transmembrane domain S6 (yellow).

2.3. Material and Methods

2.3.1. Genetic analysis

Sequencing of the *HCN4* gene in a patient with Brugada Syndrome revealed a new heterozygous base exchange in exon 4 of guanine by thymine (**G**TC → **T**TC) at the first position of the coding triplet, which resulted in an amino acid substitution of valine by phenylalanine at the position 492. This new sequence variation V492F is located in the highly conserved pore region of the cardiac ion channel and was amplified with the primers 5´-AGGTTGAGGTGAGTAGGTGGCAGG-3´ and 5´-CTGAAACTCAGATTCTCATCTCAGAGG-3´ in a 25 µl reaction solution containing 50 ng DNA, 10 µM of each primer, 2 mM dNTPs and polymerase chain reaction buffer with 5U Taq Gold polymerase. After an initial denaturation step of 5 minutes at 95°C, 30 cycles were performed (95°C for 30 sec, 62°C for 30 sec and 72°C for 45 sec), followed by a final extension of 10 minutes at 72°C. Sequencing was conducted as previously described (chapter 1) using an ABI Prism 3130 Genetic Analyzer from Applied Biosystems. A control group of 100 samples from healthy persons was examined to exclude DNA polymorphism.

2.3.2. Molecular cloning of the *HCN4* gene

The pEGFP-C1 vector with human *HCN4* cDNA was kindly provided by Prof. Gerhard Thiel from the Technical University of Darmstadt, (Darmstadt, Germany). To introduce the novel HCN4-V492F point mutation and three other variants (V492A, V492D and V492R), site-directed mutagenesis was performed (QuikChange® II XL Site-Directed Mutagenesis Kit, Stratagene, Agilent Technologies). The mutations were confirmed by direct sequencing via Eurofins.

2.3.3. Cell culture of HEK293 cells

Human embryonic kidney cells (HEK293) were cultivated in Dulbecco´s Modified Eagle Medium (DMEM/ Ham´s F-12, Biochrom AG, Berlin, Germany) supplemented with 2mM glutamine, 10% fetal calf serum (Sigma-Aldrich GmbH, Taufkirchen, Germany) and 1% penicilline/streptomycine solution (Sigma-Aldrich GmbH, Taufkirchen, Germany). The cells propagated in 25 cm^2 cell culture flasks under standard conditions in 5% CO_2 at 37°C and were passaged twice a week by using phosphate buffered saline (PBS, Sigma-Aldrich GmbH, Taufkirchen, Germany) for washing and 1%

trypsin/EDTA solution (Sigma-Aldrich GmbH, Taufkirchen, Germany) or accutase (PAA, GE Health Care, Freiburg, Germany) for enzymatic detachment of the cells. The enzymatic reaction was stopped by using the culture medium aforementioned. For the patch clamp measurements, the cells were transferred to 35 mm plates and transfected with 1 µg plasmid DNA after a confluent growing of 70%. The used transfection reagent TurboFect (Thermo Fisher Scientific Inc., Waltham, USA) was applied according to the manufacturers protocol. One day after transfection the cells were isolated and transferred in different concentrations (0.2 / 0.3 / 0.4 ml, depending of the density of cells) to new 35 mm plates with 2 ml medium. One day later the cells were used for patch clamp recordings.

2.3.4. Electrophysiological measurements in HEK293 cells

Before starting the electrophysiological measurements, the successful transfection of the cells had to be checked by visualization of the coexpressed green fluorescent protein (pE**GFP**-C1 vector). After that, the patch clamp recordings were performed (two days after transfection) in the whole-cell configuration by using an EPC-9 amplifier and the Patch Master software from HEKA Electronics (Lambrecht, Germany). The extracellular bath solution contained 110 mM NaCl, 30 mM KCl, 1.8 mM $CaCl_2$, 0.5 mM $MgCl_2$, 5 mM HEPES (pH 7.4) and the intracellular pipette solution 10 mM NaCl, 130 mM KCl, 1 mM EGTA, 0.5 mM $MgCl_2$, 5 mM HEPES (pH 7.2), 2 mM ATP, 0.1 mM GTP and 5 mM phosphocreatine. The currents were measured at room temperature and provoked according to a standard protocol (figure 19 A).

2.3.5. Statistics and data analysis

The electrophysiological data were analyzed with Patchmaster- and Fitmaster software (HEKA, Lambrecht, Germany) as well as Microsoft Excel. The instantaneous currents were recorded in the first 1% of the test voltages after decay of the capacitive artifact. The slow activation currents were measured in the last 2% of the 5 sec long test pulse. Graphics of the responding currents and the I/V relationships were displayed by Igor Pro 6.03 software (WaveMetrics, Lake Oswego, OR). The statistical significance of the results was evaluated using the Student *t*-test.

2.4. Results

2.4.1. Functional expression of HCN4-WT and HCN4-V492F mutant in HEK293 cells

For the electrophysiological investigation of the novel *HCN4* mutation, we transiently expressed the wildtype (WT) and the mutant channel in HEK293 cells and measured the currents with the patch clamp technique. Cells were therefore challenged with a voltage protocol from a holding potential at -30 mV to 5 sec long hyperpolarizing test voltages between -30 mV and -140 mV in 10 mV increments (figure 19 A); in a final step cells were then clamped to a post voltage at -30 mV. Figure 19 B-D shows the typical current responses of an untransfected HEK293 cell and of two cells expressing either HCN4-WT or the mutant HCN4-V492F, respectively. The untransfected cell shows the typical current voltage relation of HEK293 cells, which reveals a very low and linear conductance at negative voltages. The cell expressing HCN4-WT shows, in response to the same protocol, large inward currents. The results of these measurements are similar to those reported for the transient expression of HCN4-WT in HEK293 cells. Negative voltages elicit a current response with two kinetic components, an instantaneous and a slow activating component. A plot of the steady state current as a function of the clamp voltage reveals the typical current/voltage (I/V) relation of the inward rectifying HCN4-WT channel (figure 19 E).

The current responses of the cell, which expressed the homomeric V492F mutant channels, were different from that recorded in untransfected cells but also different from that of HCN4-WT expressing cells. The exemplary data show that test voltages elicit in cells, which express the mutant, also small currents with a biphasic characteristic similar to that of the WT channel at very negative values. The steady state I/V relation of the respective cell exhibits the onset of inward rectification (figure 19 E). At this point it is important to mention that cells, which express the mutant channel, could not be clamped to voltages more negative than about -110 mV. The exemplary data in figure 20 show that more negative clamp voltages generally caused an electrical collapse of the membrane. The mechanism, which is underlying this phenomenon, cannot be explained here. But it is important to mention that this phenomenon is closely connected to the mutant channel. Cells expressing the HCN4-WT or untransfected cells could be easily clamped to much more negative voltages (-140 mV) without electrical breakdown.

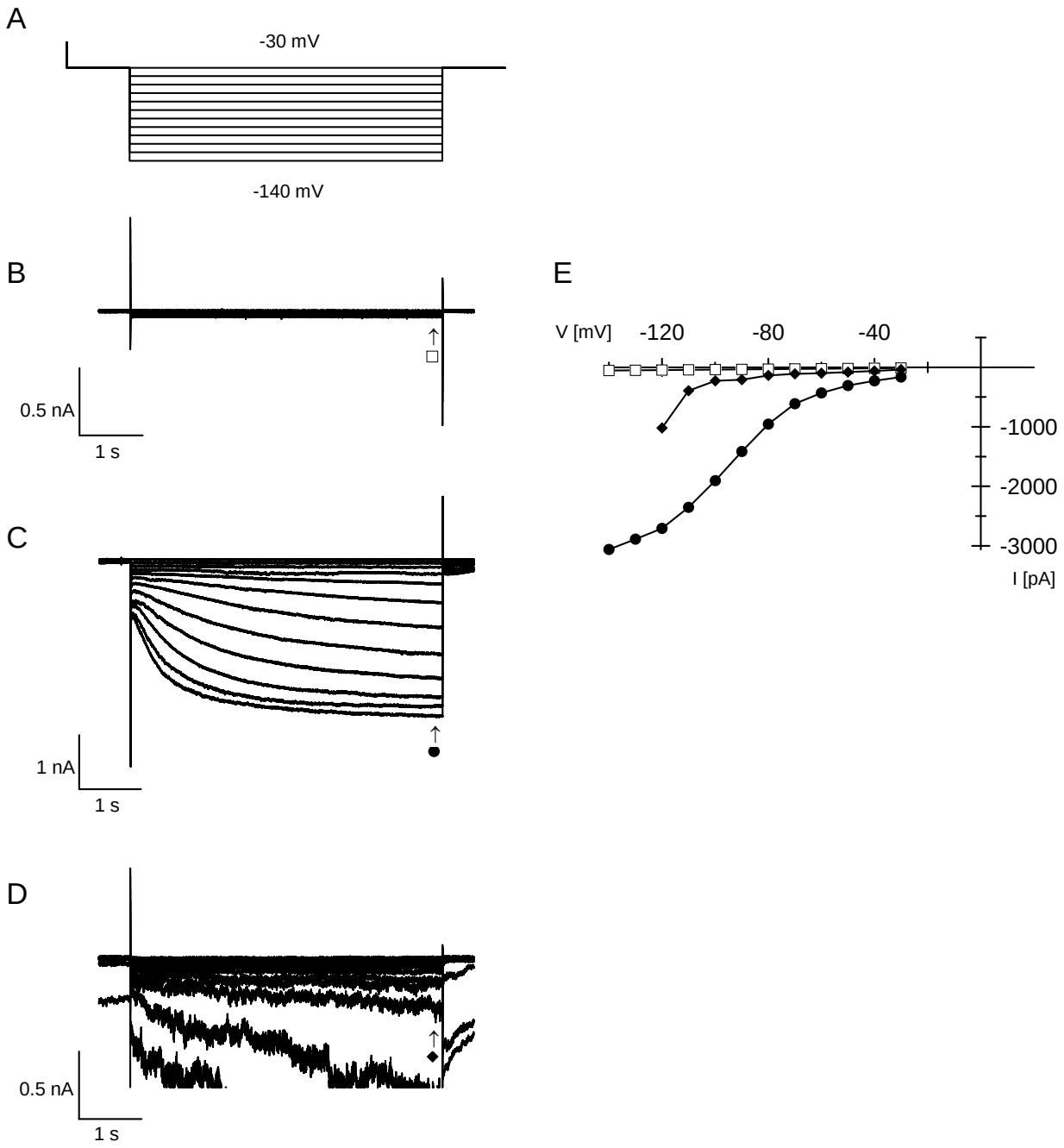

Figure 19: Expression of HCN4-WT and HCN4-V492F homotetramer in HEK293 cells.

(A) Used voltage protocol. Holding potential was -30 mV and currents were elicited by 5-second hyperpolarizing voltage steps between -30 mV and -140 mV in 10 mV increments. Currents recorded from an untransfected HEK293 cell **(B)**, a transfected cell with DNA of HCN4-WT **(C)** and DNA of HCN4-V492F **(D)**. **(E)** I/V relationship of HCN4-WT, HCN4-V492F and an untransfected HEK cell.

□ = untransfected HEK293 cell; ● = HCN4-WT; ♦ = HCN4-V492F.

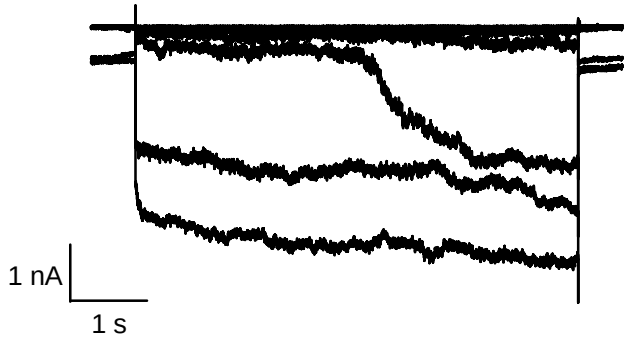

Figure 20: Expression of HCN4-V492F homotetramer in a HEK293 cell.
Impulse of more than -110 mV voltages caused electrical breakdown of the membrane potential.

To investigate the importance of the amino acid valine at the position 492 in the HCN4 protein, valine was substituted by three other amino acids: alanine, aspartic acid and arginine, which were chosen because of their different physicochemical properties. Alanine is significantly smaller than valine, whereas aspartic acid has nearly the same size but is polar. The amino acid arginine is highly polar and is significantly larger than valine. Valine and alanine are both hydrophobic amino acids, whereas arginine and asparatic acid are hydrophilic.

The respective mutants were expressed in HEK293 cells and analyzed as shown in figure 19. The results of typical recordings are presented in figure 21. It appears that all three amino acid substitutions caused the same electrophysiological pattern as the V492F mutation in the HCN4 channel (figure 21). The current responses and the corresponding steady state I/V relations show that negative voltages are in fact able to elicit an inward rectifying conductance. At close scrutiny it is apparent that the currents are biphasic with an instantaneous and a slow time dependent component.

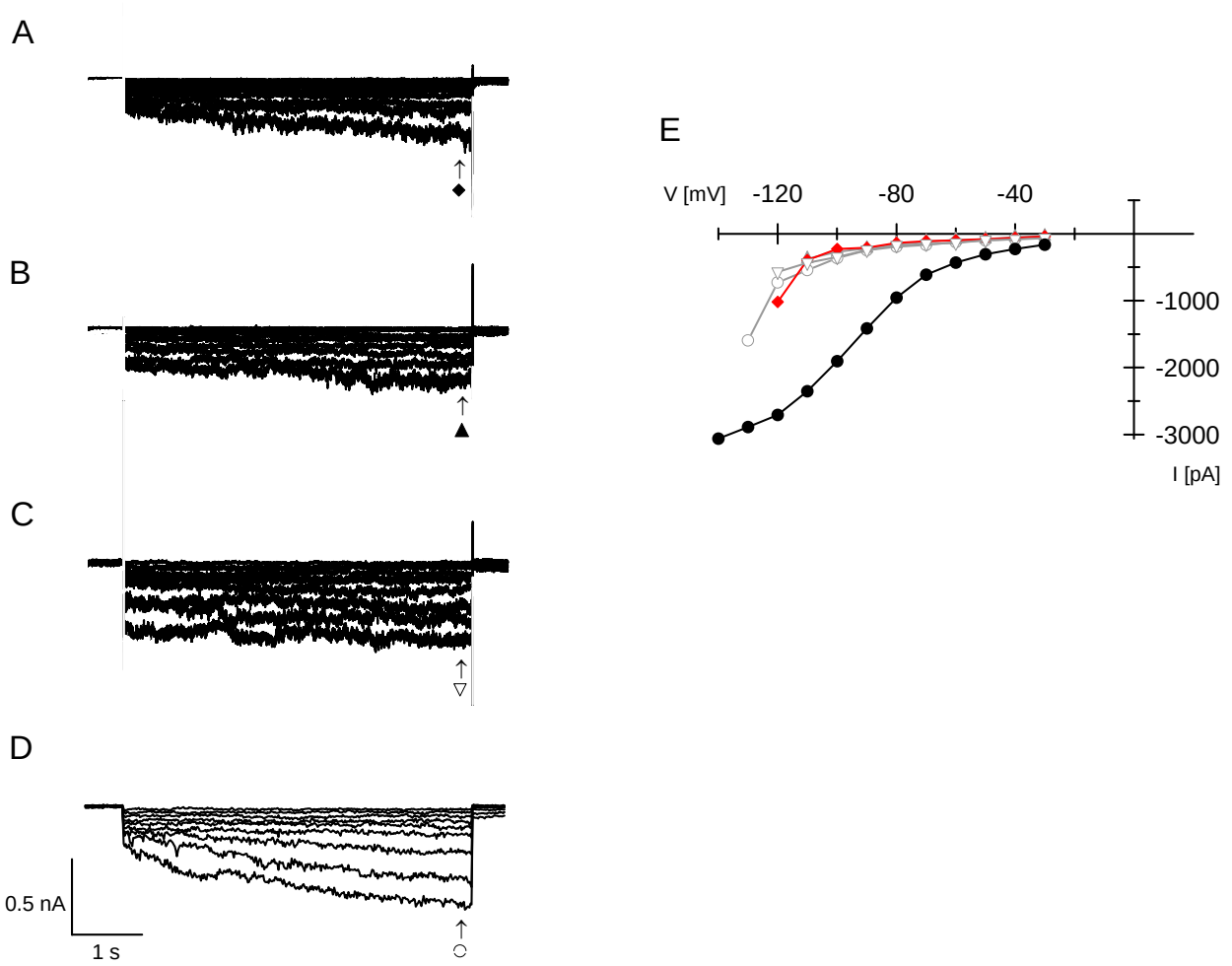

Figure 21: Expression of HCN4-V492F and three other homomeric amino acid substitutions in HEK293 cells.

Expression of **(A)** HCN4-V492F**, (B)** HCN4-V492D, **(C)** HCN4-V492R and **(D)** HCN4-V492A. **(E)** I/V relationship of HCN4-WT in comparison with all four mutants. Data of HCN4-V492F (emphasized in red) and HCN4-WT are the same like in figure 19.

♦ = HCN4-V492F; ▲ = HCN4-V492D; v = HCN4-V492R; ○ = HCN4-V492A; ● = HCN4-WT.

In this study we analyzed the data of the currents at two voltages, -90 mV and -110 mV. Both HCN4-WT and the homotetramer of V492F showed higher time dependence at the voltage of -110 mV as at -90 mV (figure 22).

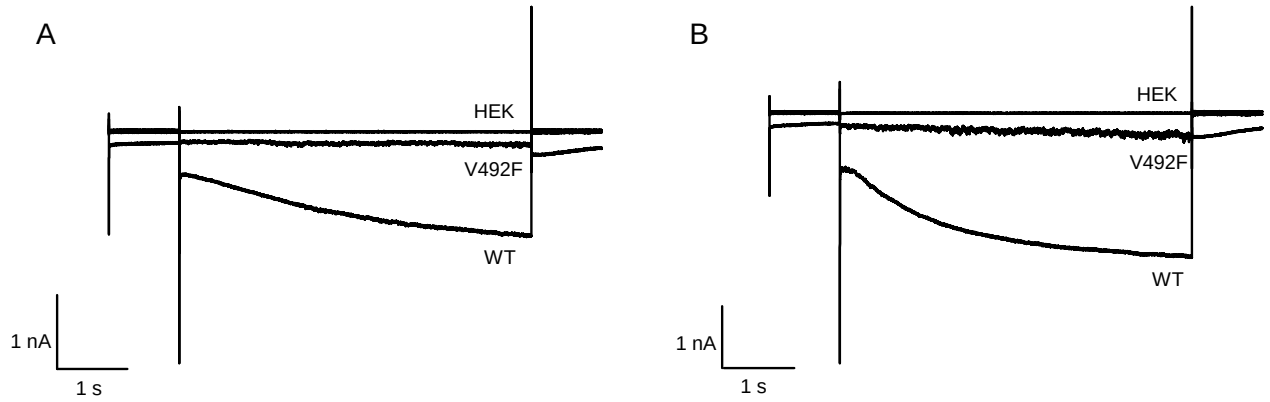

Figure 22: Time dependence of the currents of HEK, HCN4-WT and V492F.
(A) Time dependence at a voltage of -90 mV and **(B)** at a voltage of -110 mV.

2.4.2. Further electrophysiological investigations and statistical analysis

To examine the significance of the phenomena, which were presented on the basis of single cells, we analyzed the currents of a large number of HEK293 cells expressing the different channels. As a reference clamp voltage we used -90 mV, because this voltage allows a robust recording of activity of all channels without the aforementioned electrical breakdown. The study on untransfected HEK293 cells, which were used as a control, included measurements of 7 individual cells with a mean current of -45 ± 42 pA at -90 mV. In 8 HEK293 cells, which expressed the HCN4-WT channel, a mean current of -785 ± 583 pA was recorded. This difference in currents is highly significant with a score of $p<0.01$. The mutation V492F was expressed in 14 cells and was measured at the reference voltage of -90 mV showing a mean current of -196 ± 110 pA. This is significantly more current than measured in the untransfected control cells ($p<0.001$), but less than in cells expressing the HCN4 WT channel. Similar data were obtained with the other mutants. The mean currents of HEK293 cells expressing the HCN4 channel with the mutations V492A (n=7) or V492D (n=8) were about -230 ± 117 pA. This value is also significantly higher than that of the untransfected control cells ($p<0.01$). The HCN4 channel with the V492R mutation was analyzed in 15 cells and a mean current of -138 ± 114 pA was measured. This value is, albeit with a lower p value ($p<0.05$), still significantly different from that of the untransfected cells. The data including information on the cell to cell variability of the untransfected HEK293 cells and those with various HCN4 channel mutants are summarized in figure 23.

It can be concluded that all mutations at position 492 in the HCN4 protein generate active channels. However, any deviation from the WT sequence results in an impressive decrease in channel current.

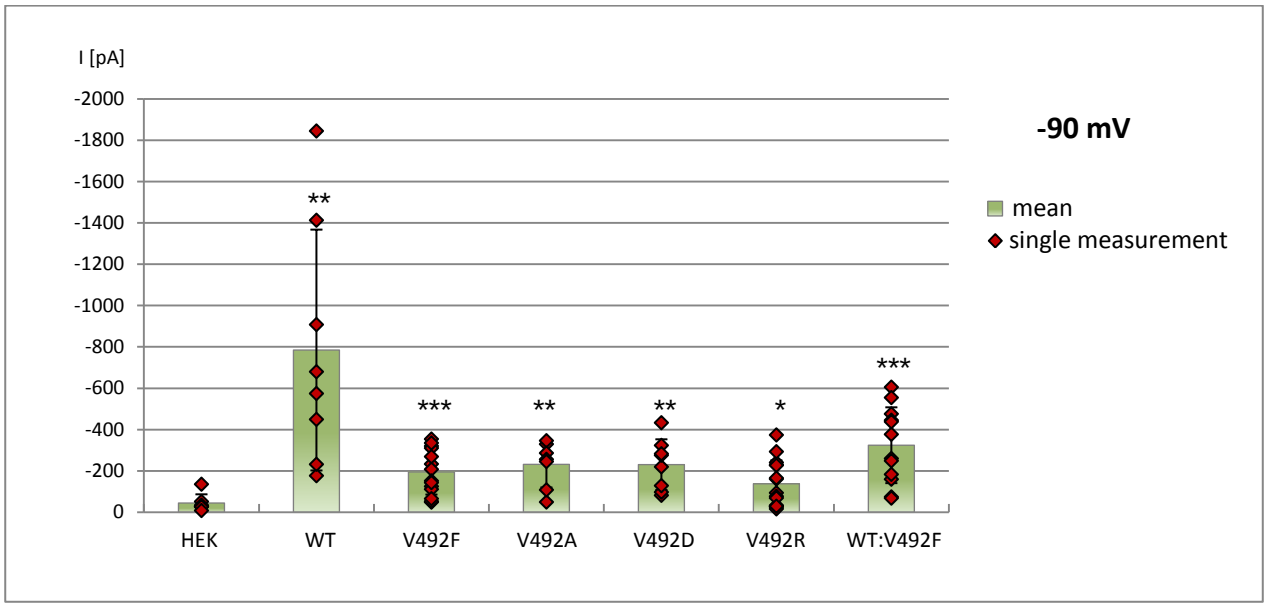

Figure 23: Histogram showing the current amplitudes recorded at a voltage step of -90 mV.
HEK n=7, WT n=8, V492F n=14, V492A n=7, V492D n=8, V492R n=15, WT:V492F (1:1) n=12.
Significance related to untransfected HEK293 cells: * $p<0.05$; ** $p<0.01$; *** $p<0.001$.

The data were also analyzed for currents at -110 mV. This has the advantage that more of the inward rectifying characteristics of the HCN channel are shown. The disadvantage of this analysis is that only a low number of cells can be considered because of the electrical breakdown at negative voltages. The data obtained from the available cells are presented in figure 24. However, the significance of the differences regarding the current amplitudes of the HCN4 mutants V492F/-A/-D/-R to HCN4-WT measured at the voltage of -90 mV was $p<0.05$ and at -110 mV $p<0.01$.

Additionally, we estimated HEK293 cells, which were transfected with the DNA of HCN4-WT as well as DNA of HCN4-V492F (1:1). According to the proportional distribution of the HCN4-WT and V492F mutated subunits in the channel, the channel conductance will be affected differently. In this study, the heterozygous cells could be divided into two populations: half of the HEK293 cells expressing heterozygous channels had an activation curve like that of the HCN4-WT and the other half like that of the HCN4-V492F channel. The mean current reached nearly the half of the WT mean value with a significance of $p<0.001$ at both voltages.

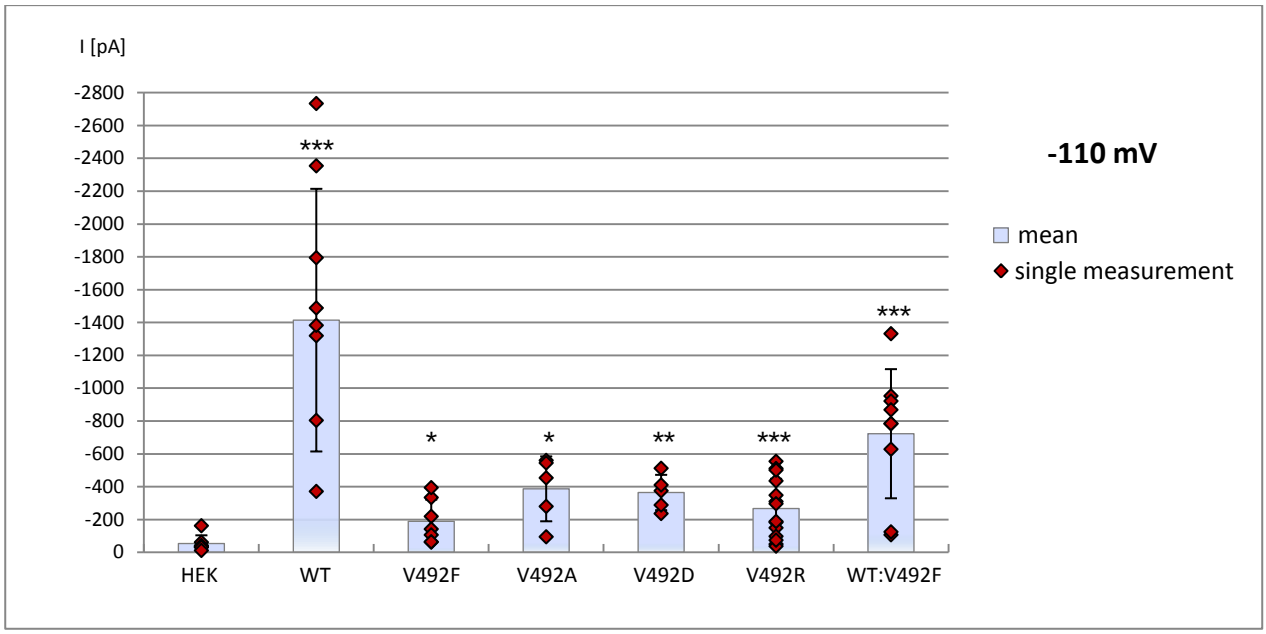

Figure 24: Histogram showing the current amplitudes recorded at a voltage step of -110 mV.

HEK n=7, WT n=9, V492F n=7, V492A and V492D n=5, V492R n=14, WT:V492F (1:1) n=9.

Significance related to untransfected HEK293 cells: * p<0.05; ** p<0.01; *** p<0.001.

The current responses of HEK293 cells expressing HCN4-WT channels and its mutants show that at negative voltages currents are activated in a biphasic manner, with an instantaneous current (Iinst) and a time dependent component (Itd). In order to understand, whether the respective mutation is affecting the slow or the instantaneous gating of the channel, we separated the steady state current at -90 mV and at -110 mV into the two kinetic components. The data shown in figure 25 and 26 indicate that the HCN4-WT current is dominated by the slow component. The situation is the opposite in the case of the mutants, which all show at the respective voltages mainly instantaneous activating currents. These instantaneous currents are significantly larger than the respective currents in untransfected cells. This indicates that a large proportion of these instantaneous currents are carried by the mutant channels. It is interesting to note that the relative contribution of the slow activating current increases in all mutants from -90 mV to -110 mV. This is consistent with the view that all mutants are able to generate a HCN like channel. The main impact of the mutations seems to be the reduction of the slow activating component of the channel.

At both voltages, the biphasic pattern of the HEK293 cells expressing the heterzogous HCN4 channel (WT:V492F) shows also a significant larger instantaneous activating current than in untransfected cells. Like the mutants, the slow activating current of heteromeric channels is predominant at a voltage of -110 mV than -90 mV. Therefore, the slow activating current increases at more negative voltage as well.

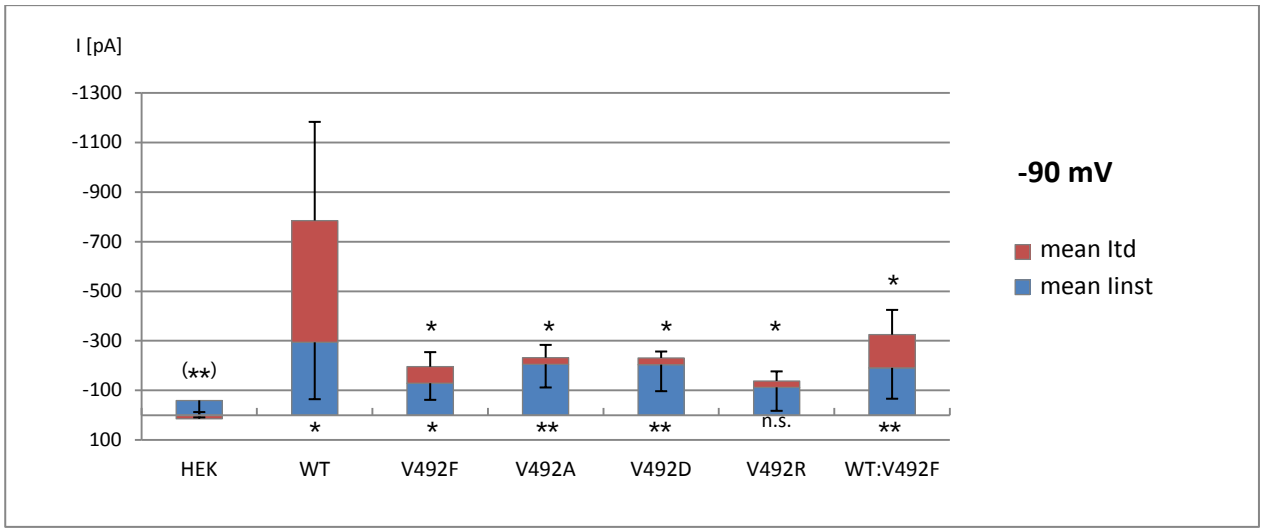

Figure 25: Histogram showing the relationship of Iinst and Itd in HEK293 cells at a voltage step of -90 mV.
Significance of the mean values of the instantaneous currents (Iinst) to the control (HEK293 cells) are below and the significance of the mean values of the time dependent currents (Itd) to HCN4-WT above.
(n.s.= not significant, * p<0.05; ** p<0.01; *** p<0.001).

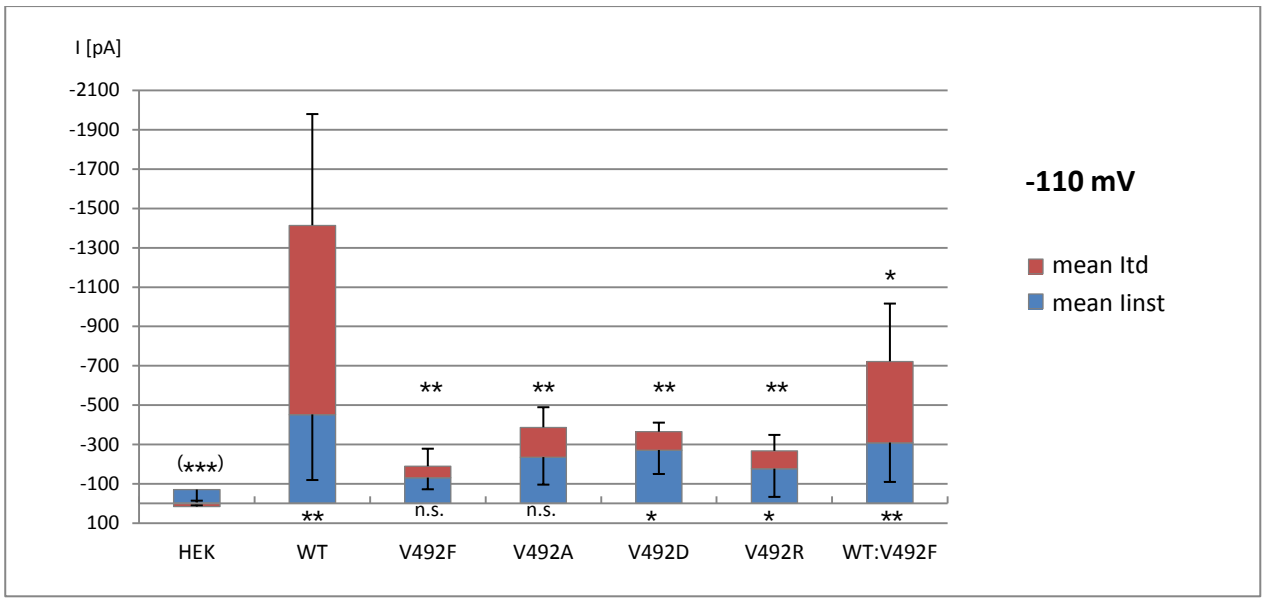

Figure 26: Histogram showing the relationship of Iinst and Itd in HEK293 cells at a voltage step of -110 mV.
Significance of the mean values of the instantaneous currents (Iinst) to the control (HEK293 cells) are below and the significance of the mean values of the time dependent currents (Itd) to HCN4-WT above.
(n.s.= not significant, * p<0.05; ** p<0.01; *** p<0.001).

2.5. Discussion

We describe here the new *HCN4* mutation V492F, which was detected in a patient with diagnosis of Brugada Syndrome (BrS). BrS is a familial disease with an autosomal dominant inheritance, which is caused by abnormalities in genes like *HCN4* [1,10,11]. *HCN4* encodes each of the four subunits of the corresponding HCN4 channel. Each subunit consists of six transmembrane domains (S1-S6) and a cyclic nucleotide-binding domain (CNBD) at the COOH terminus [12]. The domain of the protein between the transmenbrane domains S5 and S6 determines the highly conserved pore region with the ion selectivity filter. The new mutation V492F is located in the area between the filter and the S6 domain (figure 27). Some amino acid substitutions upstream of position 492 constitute mutations, which had been identified as critical amino acids; alterations of these amino acids resulted in a functional modification of the HCN channel with a reduced channel conductance [6-9].

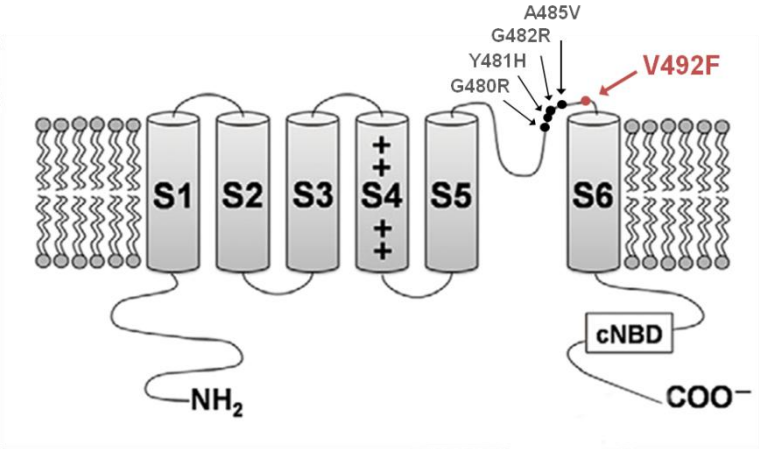

Figure 27: Schematic topology of the HCN4 protein.
Locations of the mutations are shown by arrows.
Modified from Zhou *et al.*, 2014 [12].

Several results of the present study suggest that the new V492F substitution has also a functional consequence and is not a silent polymorphism. First of all the mutation was not detected in 100 samples of healthy individuals as control. Second, the alteration is located in an evolutionary conserved region of the channel pore and third, the replacement of valine by phenylalanine is a change of two amino acids with different volume and mol-weight. Valine has a van-der-Waals volume of 105 and a weight of 43.09 g/mol, whereas phenylalanine has a van-der-Waals volume of 135 and a weight of 91.13 g/mol. Only the mol-weight of phenylalanine is more than the double of that of valine, which may affect the activity of the channel.

Our functional studies on HEK293 cells confirmed that the new V492F mutation causes a reduced channel conductance. The current responses of the cells, which express the homomeric V492F mutated channel, showed at negative voltages a smaller biphasic current than cells, which expressed the HCN4-WT channel. Since this current is still larger than that of untransfected cells, we can conclude that the mutant channel is able to conduct currents, but that the conductance is reduced (figure 19 B-D). By analyzing the two kinetic components of the currents, we observed that the instantaneous current of the mutated channel was significantly larger than the respective current in untransfected cells. This indicates that the mutant channel has a strongly altered gating. While the conductance of the WT channel is the sum of a small instantaneous and a large slow activating component, the situation is inversed in the mutant. Here the slow component becomes small and the instantaneous component dominates the conductance.

The same functional phenotype of the mutant V492F was also observed in cells expressing the other three mutated channel variants (V492A/-D/-R) at position 492. The results of these experiments support the assumption that no other amino acid with different properties as valine can preserve the functional activity of the cardiac channel HCN4. Therefore, valine is an essential amino acid at protein position 492 in the conserved pore region. This finding is in agreement with the conservation of this amino acid in HCN4 channels (figure 17).

In the present case, the mutation carrier was an 18 years old male with a typical electrocardiographic pattern of BrS [13]. He was suffering syncopes at situations of rest without any structural heart abnormalities. This can be explained by reduced channel conductance according to functional impairment of the channel. But it has to be mentioned that the patient had a heterozygous base exchange, and therefore still one intact allele, which could be upregulated to express more of the HCN4-WT protein. Because of the ratio of the HCN4 subunits for one tetramer, the overexpression of the HCN4-WT may result in a milder reduction of the HCN4 current as recorded in the electro-physiological measurements. To test this theory of compensation we transfected some of the HEK293 cells with DNA of the HCN4-WT and the HCN4 mutant V492F in a ratio of 1:1. Two populations of cells were obtained: one group of cells coexpressing HCN4-WT and V492F showed currents like the HCN4-WT and the other group of cells displayed currents like the homomeric mutated channels. These differences are possibly due to a different ratio between the channel subunits of the HCN4-WT and the V492F mutant in the cells and confirmed the assumption that heteromeric channels compensate the impaired channel protein.

Milano *et al.* [7] and Schweitzer *et al.* [8] recently reported the development of structural cardiac abnormalities as the noncompaction cardiomyopathy in association with *HCN4* mutations. In the present study, we were not able to confirm these observations based on clinical findings only in the

family with Brugada Syndrome. The morphological examinations of the index patient revealed no structural abnormalities in the heart. Additionally, the parents of the patient were asymptomatic and did not show any signs of illness. Their electrocardiogram exhibited no pathological alterations as well. They declined further investigations including genetic testing.

Although we do not know whether they are mutation carriers or not, the possibility of heteromeric HCN4 channels could be the reason for the different phenotypes within a family with BrS. The heteromerization of HCN4 and HCN2 subunits (the dominant mRNA transcript in the atrial myocardium [14]) would be a further explanation, which may underlie the benign prognosis of family members. Because the ability of rescue of impaired HCN2 channels by HCN4 subunits have been previously reported [15]. Nevertheless, genetic testing plays an important role to identify mutation carriers in families with sinus node dysfunction for the differentiation between affected or non-affected individuals and is highly recommended [16,17].

2.6. References

[1] R. Brugada, O. Campuzano, G. Sarquella-Brugada, J. Brugada, P. Brugada, Brugada syndrome, Methodist Debakey Cardiovasc J 10 (2014) 25–28.

[2] M. Biel, C. Wahl-Schott, S. Michalakis, X. Zong, Hyperpolarization-Activated Cation Channels: From Genes to Function, Physiological Reviews 89 (2009) 847–885.

[3] M. Baruscotti, A. Barbuti, A. Bucchi, The cardiac pacemaker current, J. Mol. Cell. Cardiol. 48 (2010) 55–64.

[4] D. DiFrancesco, Funny channel gene mutations associated with arrhythmias, The Journal of Physiology 591 (2013) 4117–4124.

[5] A. Verkerk, R. Wilders, Pacemaker Activity of the Human Sinoatrial Node: An Update on the Effects of Mutations in HCN4 on the Hyperpolarization-Activated Current, IJMS 16 (2015) 3071–3094.

[6] E. Nof, D. Luria, D. Brass, D. Marek, H. Lahat, H. Reznik-Wolf, E. Pras, N. Dascal, M. Eldar, M. Glikson, Point Mutation in the HCN4 Cardiac Ion Channel Pore Affecting Synthesis, Trafficking, and Functional Expression Is Associated With Familial Asymptomatic Sinus Bradycardia, Circulation 116 (2007) 463–470.

[7] A. Milano, A.M. Vermeer, E.M. Lodder, J. Barc, A.O. Verkerk, A.V. Postma, I.A. van der Bilt, M.J. Baars, P.L. van Haelst, K. Caliskan, Y.M. Hoedemaekers, S. Le Scouarnec, R. Redon, Y.M. Pinto, I. Christiaans, A.A. Wilde, C.R. Bezzina, HCN4 Mutations in Multiple Families With Bradycardia and Left Ventricular Noncompaction Cardiomyopathy, Journal of the American College of Cardiology 64 (2014) 745–756.

[8] P.A. Schweizer, J. Schröter, S. Greiner, J. Haas, P. Yampolsky, D. Mereles, S.J. Buss, C. Seyler, C. Bruehl, A. Draguhn, M. Koenen, B. Meder, H.A. Katus, D. Thomas, The Symptom Complex of Familial Sinus Node Dysfunction and Myocardial Noncompaction Is Associated With Mutations in the HCN4 Channel, Journal of the American College of Cardiology 64 (2014) 757–767.

[9] A. Laish-Farkash, M. Glikson, D. Brass, D. Marek-Yagel, E. Pras, N. Dascal, C. Antzelevitch, E. Nof, H. Reznik, M. Eldar, D. Luria, A Novel Mutation in the HCN4 Gene Causes Symptomatic Sinus Bradycardia in Moroccan Jews, Journal of Cardiovascular Electrophysiology 21 (2010) 1365–1372.

[10] K. Ueda, Y. Hirano, Y. Higashiuesato, Y. Aizawa, T. Hayashi, N. Inagaki, T. Tana, Y. Ohya, S. Takishita, H. Muratani, M. Hiraoka, A. Kimura, Role of HCN4 channel in preventing ventricular arrhythmia, J Hum Genet 54 (2009) 115–121.

[11] G. Lippi, M. Montagnana, T. Meschi, I. Comelli, G. Cervellin, Genetic and clinical aspects of Brugada syndrome: an update, Adv Clin Chem 56 (2012) 197–208.

[12] J. Zhou, W.-G. Ding, T. Makiyama, A. Miyamoto, Y. Matsumoto, H. Kimura, Y. Tarutani, J. Zhao, J. Wu, W.-J. Zang, H. Matsuura, M. Horie, A Novel HCN4 Mutation, G1097W, Is Associated With Atrioventricular Block, Circ J 78 (2014) 938–942.

[13] A.A. Wilde, Proposed Diagnostic Criteria for the Brugada Syndrome: Consensus Report, Circulation 106 (2002) 2514–2519.

[14] A. Ludwig, X. Zong, J. Stieber, R. Hullin, F. Hofmann, M. Biel, Two pacemaker channels from human heart with profoundly different activation kinetics, EMBO J. 18 (1999) 2323–2329.

[15] B. Much, C. Wahl-Schott, X. Zong, A. Schneider, L. Baumann, S. Moosmang, A. Ludwig, M. Biel, Role of Subunit Heteromerization and N-Linked Glycosylation in the Formation of Functional Hyperpolarization-activated Cyclic Nucleotide-gated Channels, Journal of Biological Chemistry 278 (2003) 43781–43786.

[16] C. Antzelevitch, Brugada Syndrome: Report of the Second Consensus Conference: Endorsed by the Heart Rhythm Society and the European Heart Rhythm Association, Circulation 111 (2005) 659–670.

[17] E. Arbelo, J. Brugada, Risk Stratification and Treatment of Brugada Syndrome, Curr Cardiol Rep 16 (2014).

2.7. Appendix

2.7.1. pEGFP-C1 vector map

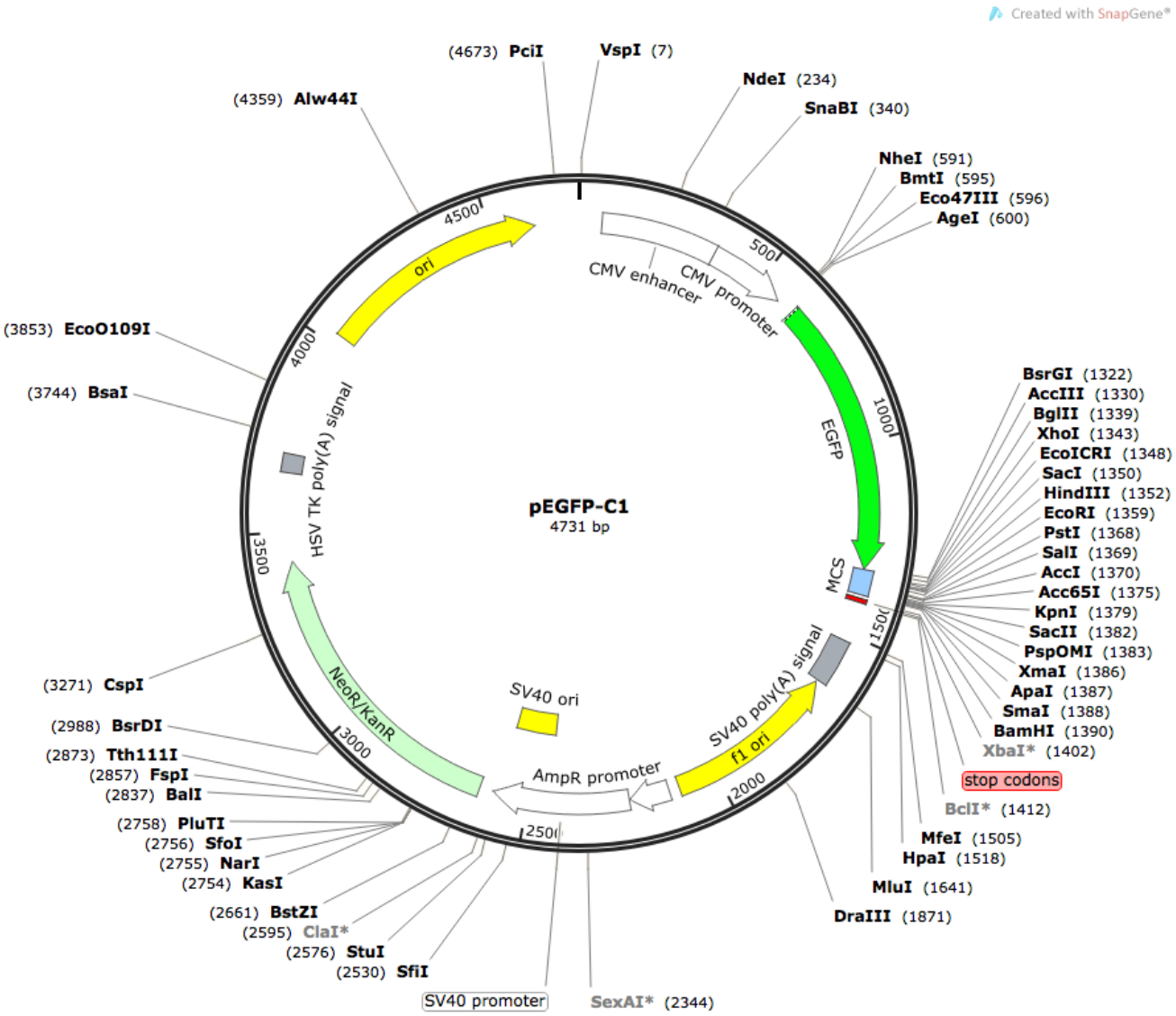

Figure 28: Plasmid map of pEGFP-C1.

Source: www.snapgene.com.

2.7.2. Mutagenesis primer

Table 3: Mutagenesis primer for HCN4-V492F.

Mutagenesis primer for HCN4-V492F	
forward	5´-GTG GGC ATG TCC GAC **T**TC TGG CTC ACC ATG-3´
reverse	5´-CAT GGT GAG CCA GA**A** GTC GGA CAT GCC CAC-3´

Table 4: Mutagenesis primer for HCN4-V492A.

Mutagenesis primer for HCN4-V492A	
forward	5´-GTG GGC ATG TCC GAC G**C**C TGG CTC ACC ATG-3´
reverse	5´-CAT GGT GAG CCA G**G**C GTC GGA CAT GCC CAC-3´

Table 5: Mutagenesis primer for HCN4-V492D.

Mutagenesis primer for HCN4-V492D	
forward	5´-GTG GGC ATG TCC GAC G**A**C TGG CTC ACC ATG-3´
reverse	5´-CAT GGT GAG CCA G**T**C GTC GGA CAT GCC CAC-3´

Table 6: Mutagenesis primer for HCN4-V492R.

Mutagenesis primer for HCN4-V492R	
forward	5´-GTG GGC ATG TCC GAC **CGG** TGG CTC ACC ATG-3´
reverse	5´-CAT GGT GAG CCA **CCG** GTC GGA CAT GCC CAC-3´

3.1. Abstract

A reduced channel conductance of a mutated ion channel in the plasma membrane may be due to several reasons. Mutations in a specified region of a coding gene can lead to a malfunction of the channel, impairment of protein synthesis or of trafficking the channel protein to the cell surface.
In this study we monitored the distribution of a GFP tagged HCN4-WT and of four different mutated HCN4 channels in HEK293 cells by confocal laser scanning microscopy (CLSM) to test, whether a mutation in position V492 of the HCN4 protein affects its synthesis or trafficking to the cell surface. The results of these experiments suggest that an amino acid exchange in position 492 of a HCN4 protein does not affect the synthesis and/or trafficking of the protein; the reduced current of these channels must be caused by an aberrant function of the channel protein.

3.2. Introduction

The hyperpolarization-activated cyclic nucleotide-gated channel 4 (HCN4) is a voltage-gated cation channel, which is mainly expressed in the brain and the heart [1]. HCN4 is a tetramer, in which each monomer consists of six transmembrane domains (S1-S6) including a positively charged voltage sensor (S4) and a highly conserved pore region (between S5 and S6). The cytosolic carboxyl terminus of each HCN4 subunit carries a cyclic nucleotide-binding domain (CNBD). Generally the HCN4 channel is activated by the membrane hyperpolarization and is responsible for an autonomic impulse generation by an inward permeation of Na^+ and K^+ ions [2]. The CNBD in the carboxyl terminus modulates this voltage dependency and shifts the channel activity to a more depolarized voltage upon intracellular binding of cAMP. This increases the pace of the heart beat.

In the recent study on the functional characterization of the novel HCN4-V492F mutation, which is located in the highly conserved channel pore, we found that this mutant affected the typical HCN type current when expressed in HEK293 cells. Cells, which were expressing the mutated channel HCN4-V492F or three different variants (V492A, V492D and V492R) exhibited a much smaller HCN4 type conductance than cells expressing the HCN4-WT channel (see chapter 2). Such a reduction of a current by a mutant channel may be due to several reasons: it may be related to a disturbance of channel function or it may also be the result of an impairment of protein synthesis or trafficking of the channel protein to the membrane. The fact that the mutation of interest is located in the highly conserved pore region of the HCN4 channel implies that the reason for the decreased channel

conductance is caused by a modification of channel function. However, at this point we cannot exclude an effect of the mutation on protein synthesis and/or trafficking. Indeed it has been shown for other pore mutations in HCN4 (G480R [3] and A485V [4]) that their reduced channel conductance in cells is related to an impairment of cell surface expression. On the other hand, another HCN4 mutant with the mutation G482R within the pore region exhibited no impaired cell surface expression [5]. Hence the location of a mutation in HCN channels does not provide an a priori explanation for the impact on channel function.

In order to test, whether a mutation in position V492 of HCN4 affects synthesis or trafficking of the HCN4 protein, we monitored the distribution of GFP tagged HCN4-WT and mutant channels in HEK293 cells by confocal laser scanning microscopy (CLSM). This approach allows to study the intracellular localization and the local concentration of HCN4 proteins inside HEK293 cells. In order to quantify the concentration of HCN4 channels in the plasma membrane of cells without disturbance of a GFP signal from inner membranes, we isolated small patches of the plasma membrane [6]. The results of these experiments show that a mutation in position V492 has no major impact on the concentration of HCN channels in the plasma membrane. This suggests that the reduced conductance of the V492 mutants is related to a corrupted function of the channel.

3.3. Material and Methods

3.3.1. Heterologous expression in HEK293 cells

The HEK293 cells were cultured and transfected as mentioned in chapter 2 (2.3.3). One day after transfection the cells were detached by swilling with phosphate buffered saline (PBS) and then centrifuged for 4 minutes at 2.500 rpm (Biofuge pico, Heraeus, Hanau, Germany). The resulting cell pellet was resuspended in 1 ml PBS. 300 µl of this cell suspension was transferred on a pretreated 25 mm round glass coverslip (for details see [6]), which was then placed in a 35 mm round culture dish filled with 2 ml PBS. During an incubation of 15 minutes the cells sedimented and adhered to the surface of the poly-lysine pretreated coverslip.

3.3.2. Plasma membrane preparation

After the cells were attached to a coverslip as described in 3.3.1., the PBS solution was replaced by 2 ml ice cold distilled water, in which cells were incubated for 5 minutes. As a result of this osmotic treatment the cells swelled and finally burst. By a following washing step with fresh water all cell organelles and debris were removed and only small patches of the plasma membranes, which were firmly attached to the glass surface, remained [6].

3.3.3. Confocal Laser Scanning Microscopy (CLSM)

The confocal laser scanning microscopy was performed at room temperature with a Leica TCS SP5 II Confocal System and the appending LAS AF software version 2.60 (Leica Microsystems CMS GmbH, Heidelberg). For imaging of isolated membrane patches, they have to be visualized on the coverslip with 50 ng/ml of the fluorescent marker Cellmask^{TM} Orange (Invitrogen GmbH, Karlsruhe, Germany), which were used for staining the plasma membrane of the patches [6]. The red fluorescence of Cellmask^{TM} Orange was excited by an argon laser at 514 nm and the resulting emission was detected at 570 - 670 nm. The green fluorescent protein (GFP), which was attached on the HCN4 protein, was excited at 488 nm and the emission was recorded at 500 - 530 nm. All images were acquired with a HCX PL APO CS 100x1.44 OIL UV objective. Digitized images were analyzed with the open source software ImageJ (http://rsb.info.nih.gov/ij).

3.4. Results

3.4.1. Synthesis and trafficking of WT and mutated HCN4 channels

The reduced conductance of the V492F mutant may be due to an aberrant function of the protein or alternatively to a reduced number of HCN4 proteins, which are synthesized and/or inserted into the plasma membrane. To compare the synthesis and trafficking, the WT channel and the mutants were fused to GFP and expressed in HEK293 cells. Figure 29 shows representative confocal images in the equatorial plain of HEK293 cells expressing either a GFP chimera with the HCN4-WT channel or with different mutants. The images exhibit no obvious differences; it appears as if all proteins are synthesized with the same efficiency and transferred to the plasma membrane. In all cases, a clear GFP fluorescence of the plasma membrane is visible.

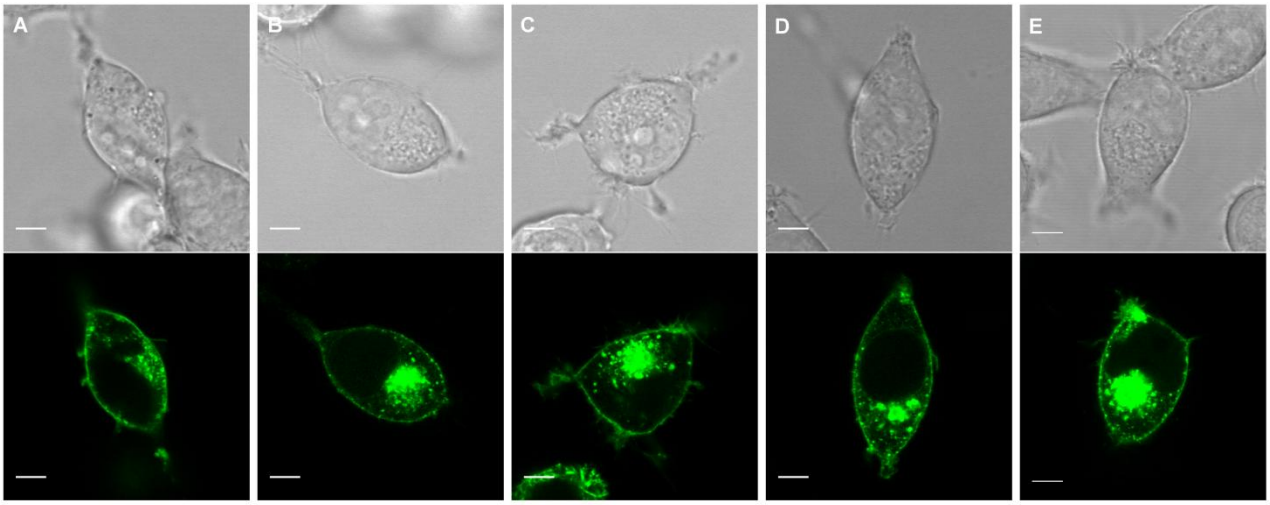

Figure 29: Confocal laser scanning microscopy of HCN4-WT and several homotetramer mutated HCN4 proteins in HEK293 cells. Above are the transmitted light and below the fluorescent images of cells transfected with DNA of **(A)** HCN4-V492A, **(B)** HCN4-V492D, **(C)** HCN4-V492F, **(D)** V492R-HCN4 and **(E)** HCN4-WT. Scale bar 5 µm.

To verify a positive location of the channels in the plasma membrane, we stained the plasma membrane with the red fluorescence marker Cellmask^{TM} Orange (Invitrogen GmbH, Karlsruhe, Germany). The overlay of both images shows that the green fluorescence of the GFP:HCN4 and the red fluorescence of the membrane co-localize (figure 30). The data confirm that the peripheral GFP staining of the HEK293 cells reports the localization of the channel proteins in the plasma membrane.

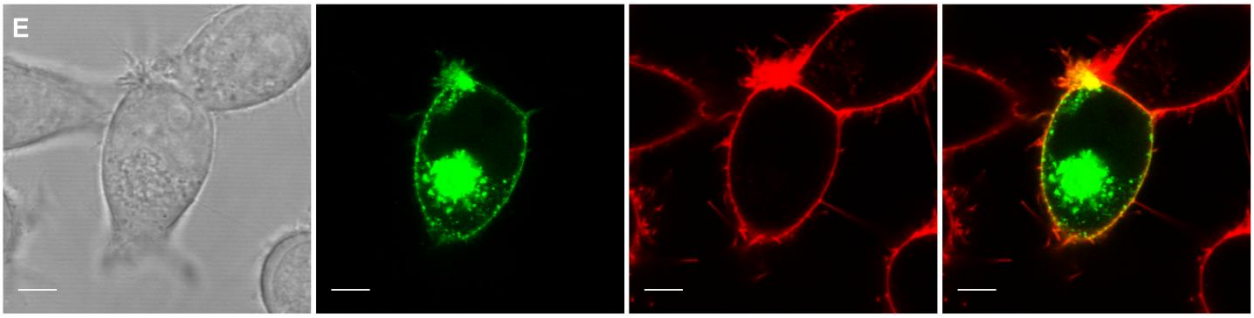

Figure 30: Confocal laser scanning microscopy of HCN4-WT using Cellmask™ Orange.
(E) the same transmitted light and fluorescent image as in figure 29 with the image of the red colored transmembrane and an overlay image of HCN4-WT. Scale bar 5 µm.

For an even better identification of the HCN4 protein in the plasma membrane we isolated small membrane patches as described by Guthmann [6]. Figure 31 shows representative images of isolated membrane patches of HEK293 cells expressing either GFP:HCN4-WT or a GFP chimera with mutants. The images show that the membrane patches, which are identified by the red fluorescence of Cellmask™ Orange, all contain GFP. The co-localization of the two fluorescent signals is evident in the top and in the side view of the confocal images. The side view of the patches confirms that only the layer of the membrane, which is attached to the coverslip, remains after the isolation procedure. The images endorse that the WT channel as well as all the different HCN4 mutants are positively transferred to the plasma membrane.

Images obtained from the isolated patches suggest that the density of the HCN4-WT and of the several mutated channels in the plasma membrane is identical. For this reason the green and the red fluorescence of a defined area in an isolated membrane patch were estimated from patches containing GFP chimera of the WT and the mutant channel V492F, respectively. Both fluorescence intensities were first normalized to the respective area. In the second step, the relative values of the green fluorescence were divided by the corresponding values of the red fluorescence. This second normalization was necessary, because the images were obtained with different laser intensities. The analysis reveals in 4 membrane patches from HEK293 cells expessing the HCN4-WT channel a relative fluorescence value of 40.4 ± 21. The same analysis of 3 patches with the mutant channel V492F reveals a relative fluorescence value of 45.2 ± 12. The result of this analysis supports the general impression from confocal images in that the mutant channels are present in the plasma membrane with the same density as the WT channel.

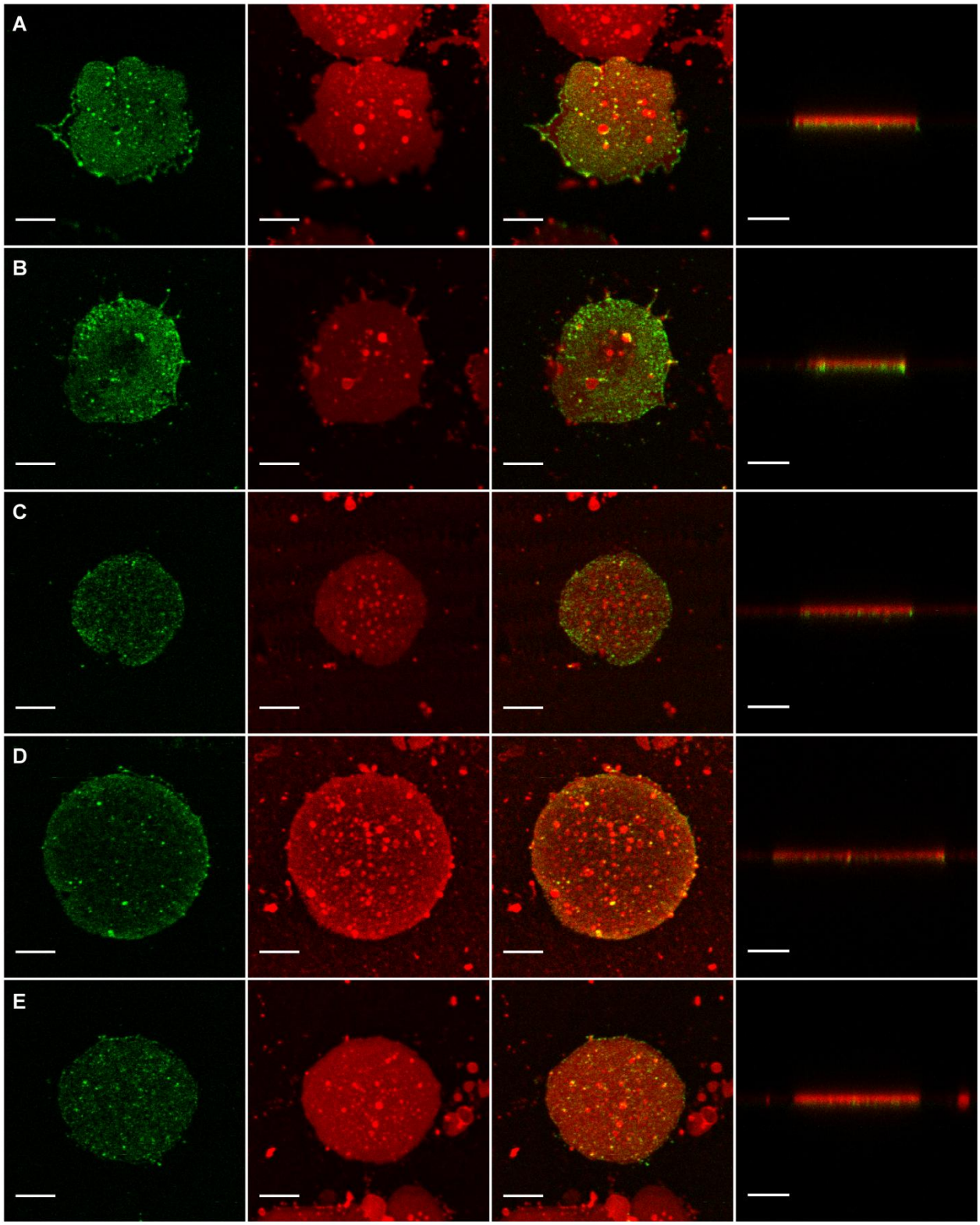

Figure 31: Napobac images of HCN4-WT and several homotetramer mutated HCN4 proteins in HEK293 transmembranes. First column are the green fluorescent HCN4 channels, second column are the red colored transmembrane patches, third column the overlay of both and the fourth a side view of **(A)** HCN4-V492A, **(B)** HCN4-V492D, **(C)** HCN4-V492F, **(D)** HCN4-V492R and **(E)** HCN4-WT. Scale bar 5 µm.

3.5. Discussion

The functional characterization of HCN4 mutants in the pore region of the channel has shown that mutations in V492 generate in HEK293 cells a much smaller inward current than the WT channel. Although the position of the mutation in the conserved pore domain of the channel suggests an impact on channel function, it cannot be excluded that the mutation may also affect protein synthesis or protein trafficking. Other studies have already shown that the pore mutation G482R in HCN4 [5] is not affecting the surface expression of the mutant in HEK293 cells. This implies that a sequence variation within the pore region is not necessarily affecting the channel synthesis or trafficking. Much *et al.* [7] also confirmed this view by demonstrating that a conserved consensus site for *N*-glycosylation in the extracellular loop between S5 and the pore helix (protein position 458) is required for an undisturbed surface expression of HCN channels. Notably this critical site is not affected by the mutation V492F. Furthermore Akhavan *et al.* [8] showed that the CNBD at the cytosolic carboxyl terminus of the channel, but not the pore region, is presumably the most important site, which determines channel trafficking to the cell surface. Still a sensitivity of channel trafficking to mutations in the pore region cannot be excluded. Two pore mutations in HCN4 (G480R [3] and A485V [4]) at a position close to 482 caused a clear reduction of the HCN current, but in that case the effect could be explained by an impairment of the cell surface expression.

In this study, we performed experiments to examine whether a mutation in position 492 causes a defective synthesis or trafficking of the HCN4 protein. When considering the fluorescence of the reporter protein GFP, which is attached to the channel as an indirect marker for the HCN4 channel, we find no appreciable difference between cells expressing the WT channel or its mutants. Using the GFP signal as a marker for the channel protein we can detect the fluorescence inside the cell and in association with the plasma membrane in all cases. The results of these experiments suggest that a mutation in position 492 has no impact on channel synthesis and trafficking. The assumption that the mutation does not affect the concentration of HCN4 channels in the membrane can be further substantiated by the analysis of isolated patches of the plasma membrane of HEK293 cells. A recently developed method allows a pure separation of the plasma membrane from the rest of the cell [6]. The benefit of this procedure is that the green fluorescence, which is associated with this membrane patch, must result from HCN4 proteins, which are inserted in the plasma membrane. This allows the exclusion of fluorescence contaminants such as of intracellular membranes like the ER or vesicles [6]. A comparative quantification of membrane patches from cells expressing the HCN4-WT or mutants shows no appreciable difference in the amount of GFP fluorescence per area of isolated plasma membrane. This indicates that the mutant channel is apparently neither impaired in synthesis nor trafficking, which supports the view that the reduced conductance of mutant channels with an amino acid exchange in position 492 is due to an aberrant function of the channel protein. Although

some effects of a mutation in this site on protein synthesis and/or trafficking cannot be completely excluded, they may play a minor role only.

3.6. References

[1] M. Baruscotti, A. Barbuti, A. Bucchi, The cardiac pacemaker current, J. Mol. Cell. Cardiol. 48 (2010) 55–64.

[2] M. Biel, C. Wahl-Schott, S. Michalakis, X. Zong, Hyperpolarization-Activated Cation Channels: From Genes to Function, Physiological Reviews 89 (2009) 847–885.

[3] E. Nof, D. Luria, D. Brass, D. Marek, H. Lahat, H. Reznik-Wolf, E. Pras, N. Dascal, M. Eldar, M. Glikson, Point Mutation in the HCN4 Cardiac Ion Channel Pore Affecting Synthesis, Trafficking, and Functional Expression Is Associated With Familial Asymptomatic Sinus Bradycardia, Circulation 116 (2007) 463–470.

[4] A. Laish-Farkash, M. Glikson, D. Brass, D. Marek-Yagel, E. Pras, N. Dascal, C. Antzelevitch, E. Nof, H. Reznik, M. Eldar, D. Luria, A Novel Mutation in the HCN4 Gene Causes Symptomatic Sinus Bradycardia in Moroccan Jews, Journal of Cardiovascular Electrophysiology 21 (2010) 1365–1372.

[5] P.A. Schweizer, J. Schröter, S. Greiner, J. Haas, P. Yampolsky, D. Mereles, S.J. Buss, C. Seyler, C. Bruehl, A. Draguhn, M. Koenen, B. Meder, H.A. Katus, D. Thomas, The Symptom Complex of Familial Sinus Node Dysfunction and Myocardial Noncompaction Is Associated With Mutations in the HCN4 Channel, Journal of the American College of Cardiology 64 (2014) 757–767.

[6] T. Guthmann, The outer transmembrane domain of the Kesv channel determines its intracellular localization: A molecular and microscopic analysis of protein sorting. 2013 PhD Thesis TU Darmstadt.

[7] B. Much, C. Wahl-Schott, X. Zong, A. Schneider, L. Baumann, S. Moosmang, A. Ludwig, M. Biel, Role of Subunit Heteromerization and N-Linked Glycosylation in the Formation of Functional Hyperpolarization-activated Cyclic Nucleotide-gated Channels, Journal of Biological Chemistry 278 (2003) 43781–43786.

[8] A. Akhavan, Identification of the cyclic-nucleotide-binding domain as a conserved determinant of ion-channel cell-surface localization, Journal of Cell Science 118 (2005) 2803–2812.

[9] M.F. Netter, M. Zuzarte, G. Schlichthörl, N. Klöcker, N. Decher, The HCN4 Channel Mutation D553N Associated With Bradycardia Has a C-linker Mediated Gating Defect, Cell Physiol Biochem 30 (2012) 1227–1240.

SUMMARY

Brugada (BrS) and Sick Sinus Syndrome (SSS) are inheritable diseases, which are characterized by different cardiac arrhythmias. Tachy- and bradycardy as well as sinoatrial block, sinus rest or cardiac arrest are clinical manifestations of these diseases, which may be detected in electrocardiograms of affected persons. Both BrS and SSS are not based only on clinical, but also on symptomatic features. Symptoms like chronotropic incompetence, dizziness, syncopes, palpitations or atrial/ ventriculare fibrillation until sudden cardiac arrest are results of such cardiac arrhythmias. The appearance and occurrence of these symptoms are phenotypic and not always existing, which makes the diagnosis of these diseases based only on clinical and symptomatic criteria very difficult.
Over the last years, a number of genetic abnormalities in genes encoding subunits of cardiac potassium, sodium and calcium channels, as well as in genes involved in the trafficking or regulation of these channels could be associated with both syndromes. Therefore, genetic screening of persons at a potential risk should be performed for diagnosing.

HCN4 is one of these genes, which could be associated with BrS and SSS. It encodes the hyperpolarization-activated, cyclic nucleotide-gated cation channel, which is crucial for the uninterrupted function of the sinoatrial node in the heart. HCN4 is one of four isoforms (HCN1-4) and is mainly expressed in the brain and the heart to generate a pacemaker impulse for autonomic activity. These channels are voltage-gated and are activated by the membrane hyperpolarization. In a ratio of 1:3 to 1:5, Na^+ and K^+ ions flow through a pore, which is formed by four subunits of the channel. As a consequence of the activity of the HCN4 channel the membrane depolarizes to the threshold voltage, which in turn triggers the subsequent action potential. Mutations in the *HCN4* gene may lead to cardiac dysfunctions, which occur in diseases such as BrS and SSS. To date, more than 23 mutations in the *HCN4* gene have been identified and associated with clinically established or potential sinus node dysfunctions.

In the present study, genetic screening of patients with suspected or diagnosed Brugada or Sick Sinus Syndrome was performed to identify new mutations in the *HCN4* gene. In the coding *HCN4* region of 62 patients, six already known and one novel sequence alteration were detected: two are located in exon 1 (N-terminus), two in exon 4 (one in the pore and one in the beginning of the C-terminus loop) and three in exon 8 (C-terminus loop). All of these six base exchanges are listed in the NCBI-database (National Center of Biotechnology) as sequence variations with no functional modification. The new sequence variant V492F was not listed in the database and is located in the highly conserved pore region of the HCN4 channel. To prove, whether this variant is a common polymorphism or a novel mutation, 100 blood samples of healthy persons were tested. None of these samples contained this new sequence variation, what suggests a new mutation.

The subsequent electrophysiological investigations on HEK293 cells expressing the HCN4-V492F mutant and three additional variants (V492A/-D/-R) at the protein position V492 indicated a reduced channel conductance in comparison to HEK293 cells expressing the HCN4-WT. This may not be exclusively attributed to a functional disorder of the channel, but may also be due to an impairment of the protein synthesis or of trafficking the channel protein to the cell surface.
To address this question, the distribution of GFP tagged HCN4-WT and of mutant channels were investigated in HEK293 cells using confocal laser scanning microscopy (CLSM). The CLSM images of HEK293 cells expressing the respective mutated channels showed the same intracellular distribution and local concentration of the HCN4 protein as the images of HEK293 cells expressing the HCN4-WT. The modified technique nabopac was additionally used to isolate plasma membrane patches from cells, which had been transfected with DNA of HCN4-WT or of the several mutated channels. These highly pure plasma membrane patches showed no differences in their GFP fluorescence intensity, which indicates that an amino acid exchange in position 492 of the HCN4 protein apparently neither impaired the synthesis nor the trafficking of the channel.

Taken together, the reduced conductance of a HCN4-V492F mutant is apparently caused only by an aberrant function of the channel protein. The reduced channel conductance explains the symptoms the mutation carrier exhibits, who is suffering from unclear syncopes in resting situations and confirms the BrS diagnosis.

GERMAN SUMMARY

Das Brugada (BrS) und das Sick Sinus Syndrom (SSS) sind vererbbare Erkrankungen, welche sich durch verschiedene kardiale Arrhythmien auszeichnen. Tachykardien und Bradykardien sowie ein sinoatrialer Block, Sinuspausen oder Herzstillstand sind klinische Manifestationen dieser Krankheiten, welche sich im Elektrokardiogramm von betroffenen Personen zeigen können. Sowohl BrS als auch SSS basieren nicht nur auf klinischen, sondern auch auf symptomatischen Eigenschaften. Symptome wie die chronotrope Inkompetenz, Schwäche, Synkopen, Herzklopfen oder atriales/ventrikuläres Flimmern bis hin zum plötzlichen Herzstillstand sind das Ergebnis solcher kardialen Arrhythmien. Das Auftreten und die Ausprägungen dieser Symptome sind phänotypisch und nicht immer existent, was die Diagnose dieser Erkrankungen nur anhand der klinischen und symptomatischen Kriterien sehr schwierig macht.
In den vergangenen Jahren konnten immer mehr genetische Anomalien in Genen, welche die Untereinheiten von Kalium-, Natrium- und Calciumkanälen kodieren, sowie in Genen, die in den Transport oder die Regulation dieser Kanäle involviert sind, mit beiden Krankheiten assoziiert werden. Ein genetisches Screening sollte daher in die Untersuchung von eventuell gefährdeten Personen mit einbezogen werden.

HCN4 ist eines der Gene, welches mit BrS und SSS assoziiert werden konnte. Es kodiert einen hyperpolarisations-aktivierten und zyklisch nukleotid-gesteuerten Kationenkanal, welcher für die reibungslose Funktion des Sinusknoten im Herzen wichtig ist. HCN4 ist einer von vier Isoformen (HCN1-4) und wird hauptsächlich im Gehirn und im Herzen exprimiert, um dort die autonome Aktivität eines Schrittmacherimpulses zu generieren. Diese Kanäle sind spannungsabhängig und werden durch die Membranhyperpolarisierung aktiviert. Natrium- und Kaliumionen strömen in einem Verhältnis 1:3 oder 1:5 durch eine Pore ein, welche durch vier Untereinheiten des Kanals geformt wird. Dadurch depolarisiert die Spannung zur der Schwelle, bei der das nächste Aktionspotentail ausgelöst wird. Mutationen im *HCN4* Gen können zu kardialen Dysfunktionen führen, welche häufig mit Krankheiten wie dem BrS oder SSS assoziiert sind. Bis heute wurden mehr als 23 Mutationen im *HCN4* Gen identifiziert und mit klinisch etablierten oder potentiellen Dysfunktionen des Sinusknotens in Verbindung gebracht.

In der vorliegenden Arbeit wurde ein genetisches Screening von Patienten mit der Diagnose oder dem Verdacht auf Brugada oder Sick Sinus Syndrom durchgeführt, um neue Mutationen im *HCN4* Gen zu identifizieren. In der kodierenden *HCN4* Region von 62 Patienten wurden sechs bereits bekannte und eine neue Sequenzabweichung detektiert: zwei befinden sich in Exon 1 (N-Terminus), zwei in Exon 4 (eine in der Pore und eine am Anfang der Schleife des C-Teminus) und drei in Exon 8 (C-Terminus). Jeder der sechs bekannten Basenaustausche ist in der NCBI Datenbank (National

Center of Biotechnologie) als eine Sequenzvariante ohne funktionelle Folge gelistet. Die neue Sequenzvariante V492F war nicht in der Datenbank aufgeführt und befindet sich in der hoch konservierten Porenregion des HCN4 Kanals. Um zu prüfen, ob es sich um einen häufigen Polymorphismus oder eine neue Mutation handelt, wurden 100 Blutproben gesunder Personen untersucht. Keine dieser Proben enthielt diese neue Sequenzvariante, was auf eine Mutation schließen lässt.

Die im Anschluss durchgeführten elektrophysiologischen Untersuchungen an HEK293 Zellen, welche die HCN4-V492F Mutante und drei weitere Varianten (V492A/-D/-R) an der Proteinposition V492 exprimierten, zeigten eine reduzierte Kanalleitfähigkeit im Vergleich zu den HEK293 Zellen, welche den HCN4-WT exprimierten. Dies lässt sich nicht ausschließlich auf eine funktionelle Störung des Kanals zurückführen, sondern könnte auch Folge einer Beeinträchtigung der Proteinsynthese oder des Transportes der Proteine zur Zellmembran sein.
Hierzu wurden GFP markierte HCN4-WT und mutierte Kanäle in HEK293 Zellen mittels konfokaler Laser-Mikroskopie (CLSM) untersucht. Die CLSM-Aufnahmen zeigten alle die gleiche zelluläre Verteilung und lokale Konzentration der mutierten als auch nicht mutierten HCN4 Proteine.
Mittels der modifizierten Technik Napobac, wurden zusätzlich Plasmamembran-Fragmente der Zellen isoliert, welche mit der DNA des HCN4-WT oder der verschiedenen mutierten Kanäle transfiziert wurden. Diese hoch reinen Membranflecken wiesen keine nennenswerte Unterschiede in ihrer GFP Fluoreszenzintensität auf, was darauf hindeutet, dass ein Aminosäureaustausch in der Position 492 des HCN4 Proteins offenbar weder die Proteinsynthese noch den Transport des Kanalproteins zur Zellmembran beeinträchtigt.

Zusammenfassend lässt sich feststellen, dass die reduzierte Leitfähigkeit der HCN4-V492F Mutante offenbar nur durch eine funktionelle Störung des Kanals verursacht wird. Die reduzierte Leitfähigkeit des HCN4 Kanals erklärt die Symptome des Mutationsträgers, welcher an unklaren Synkopen in stressfreien Situationen leidet und bestätigt den Verdacht auf Brugada Syndrom.

LIST OF ABBREVIATIONS

µl	microliter
µM	micromolar
3D	3 dimensional
A	adenine
AA	amino acid
ATP	adenosine triphosphate
BrS	Brugada Syndrome
C	cytosine
C°	degree Celsius
$CaCl_2$	calcium chloride
cAMP	cyclic adenosine monophosphate
cDNA	complementary deoxyribonucleic acid
CLSM	Confocal Laser Scanning Microscopy
cm^2	cubic centimeter
CNBD	cyclic nucleotide-binding domain
DMEM	Dulbecco´s Modified Eagle Medium
DMSO	dimethyl sulfoxide
DNA	deoxyribonucleic acid
ECG	electrocardiogram
EGFP	enhanced green fluorescent protein
EGTA	ethylene glycol tetraacetic acid
ER	endoplasmic reticulum
g	gram
G	guanine
GFP	green fluorescent protein
GTP	guanosine triphosphate
HCN (1-4)	hyperpolarization-activated, cyclic nucleotide-gated channel (1-4)
HEK293	human embryonic kidney 293 cell
HEPES	4-(2-hydroxyethyl) piperazine-1-ethanesulfonic acid
I/V	current/voltage
ICD	implantable cardioverter defibrillator
Iinst	instantaneous current
Itd	time dependent current
K^+	potassium ion
KCl	potassium chloride

$MgCl_2$	magnesium chloride
ml	milliliter
mm	millimeter
mM	millimolar
mRNA	messenger ribonucleic acid
MRT	magnetic resonance tomography
mV	millivolt
n	number
n.s.	not significant
nA	nanoampere
Na^+	sodium ion
NaCl	sodium chloride
NCBI	National Center of Biotechnology
ng	nanogram
p	probability
pA	picoampere
PBS	phosphate buffered saline
PCR	polymerase chain reaction
rpm	revolution per minute
s	second
SCN5A	sodium channel, voltage gated, type 5 alpha subunit
sec	second
SND	sinus node dysfunction
SSS	Sick Sinus Syndrome
T	thymine
U	units
WT	wildtype

LIST OF FIGURES

LIST OF TABLES

DANKSAGUNG

Für das Gelingen dieser Doktorarbeit möchte ich mich bei der DNA-Abteilung des Instituts für Rechtsmedizin Frankfurt und dem Arbeitskreis von Herrn Prof. Dr. Gerhard Thiel der Technischen Universität Darmstadt bedanken. Ohne die tolle Zusammenarbeit beider Abteilungen wäre die Umsetzung dieser Arbeit so nicht möglich gewesen.

Ganz besonders möchte ich mich bei Herrn **Prof. Dr. Gerhard Thiel** persönlich bedanken, denn er ermöglichte mir nicht nur die Durchführung der elektrophysiologischen Messungen an HEK-Zellen in seinem Arbeitskreis, sondern übernahm auch die Betreuung und Begutachtung meiner Arbeit. Für seine Unterstützung bis zu Letzt bin ich ihm sehr dankbar. Vielen Dank!

Ebenfalls möchte ich mich bei Herrn **Prof. Dr. Bodo Laube** bedanken, der sich sofort dazu bereit erklärte die Begutachtung meiner Dissertation zu übernehmen.

Für die externe Betreuung und Begutachtung meiner Arbeit möchte ich mich bei Frau **PD Dr. Silke Kauferstein** und Herrn **Prof. Dr. Dietrich Mebs** bedanken. Beide haben mich besonders gegen Ende meiner Arbeit sehr unterstützt.

Dem Direktor des Instituts für Rechtsmedizin Frankfurt, Herrn **Prof. Dr. Marcel Verhoff**, und im Besonderen seinem Vorgänger, Herrn **Prof. Dr. Hansjürgen Bratzke,** danke ich für die Ermöglichung meiner Arbeit durch das Bereitstellen sämtlicher Geräte und Materialien, die zur Erstellung meiner Dissertation nötig waren.

Für jegliche Art der Unterstützung möchte ich mich von ganzem Herzen bei meiner Freundin und Kollegin **Dipl.-Biol. Barbara Zajac** bedanken. Ohne Dich wäre ich das ein oder andere Mal verzweifelt. Danke, dass Du immer für mich da bist.

Dipl.-Biol. Tina Jenewein möchte ich für den gemeinsamen Weg und die gegenseitige fachliche und persönliche Unterstützung danken.

Auch bei dem restlichen Team der DNA-Abteilung möchte ich mich für manch offenes Ohr und den ein oder anderen Rat bedanken. Besonders den Studenten, wie **Stefanie Scheiper** gilt mein Dank, denn sie haben mich bei der Durchführung meiner Laborarbeiten sehr unterstützt.

Besonders hervorheben möchte ich jedoch **Dr. Brigitte Hertel**. Ich danke ihr von ganzem Herzen für ihre Unterstützung in sämtlichen Laborfragen und für das Nahebringen der Elektrophysiologie, sowie dessen mühsame Auswertung. Liebe Brigitte, ich danke Dir dafür, dass Du mich in manch schweren Momenten begleitet hast. Vielen Dank!!

Mein Dank gilt auch einigen Mitarbeitern der AG Thiel, die mich bei der Durchführung meiner dortigen Laborarbeit sehr unterstützt haben. Ganz besonders **Dipl.-Biol. Anne Berthold**, die viele Stunden mit mir am CLSM verbrachte. Danke.

Meiner **Familie** danke ich für ihre moralische Unterstützung, ihren Glauben an mich und das Vertrauen in meine Arbeit. Es macht mich sehr stolz Euch in jeder Lebenslage an meiner Seite zu wissen.

Ein großes Dankeschön geht an meinen Freund und Lebenspartner **Michael Wedler**, der mich durch viele Gespräche immer wieder aufgebaut und ermutigt hat. Ich danke Dir für Deine Geduld und Deine Liebe!

Zum Schluss möchte ich mich noch bei allen **Patienten** und **Kooperationspartnern** für ihre Teilnahme an dieser Studie bedanken.

EHRENWÖRTLICHE ERKLÄRUNG

Ich erkläre hiermit ehrenwörtlich, dass ich die vorliegende Arbeit entsprechend den Regeln guter wissenschaftlicher Praxis selbstständig und ohne unzulässige Hilfe Dritter angefertigt habe.

Sämtliche aus fremden Quellen direkt oder indirekt übernommenen Gedanken sowie sämtliche von Anderen direkt oder indirekt übernommenen Daten, Techniken und Materialien sind als solche kenntlich gemacht. Die Arbeit wurde bisher bei keiner anderen Hochschule zu Prüfungszwecken eingereicht.

Darmstadt, den 29.05.2015

_____

Dipl.-Biol. Stephanie Biel

Persönliche Daten

Name:	Stephanie Biel
Geburtstag:	06.03.1986
Geburtsort:	Pinneberg
Staatsangehörigkeit:	deutsch
Familienstand:	ledig

Ausbildungsdaten

seit 2013	**Promotion** (Dr. rer. nat.) Technische Universität Darmstadt Fachbereich Biologie
2005 - 2011	**Studium** Johann Wolfgang Goethe Universität Frankfurt am Main Studiengang: Diplom Biologie Abschluss: Diplom Biologin (Note: „sehr gut“)
2002 - 2005	**Wirtschaftsgymnasium** Johann-Philipp-Bronner Wirtschaftsgymnasium Wiesloch (Rhein-Neckar-Kreis) Abschluss: Allgemeine Hochschulreife (Note: 2,7)
1996 - 2002	**Realschule** Theodor-Heuss-Realschule Walldorf (Rhein-Neckar-Kreis) Abschluss: Mittlere Reife
1992 - 1996	**Grundschule** in Lienen (Westfalen), Mondsee (Österreich) und St. Leon (Rhein-Neckar-Kreis)

Berufliche Erfahrungen und Tätigkeiten

2000 (Frühjahr)	Schüleraustausch in England
2000 (Winter)	Schüleraustausch in USA
2001	Praktikum in der Eulen Apotheke St. Leon
2005	Spanischsprachkurs in Marbella, Spanien
2009	Tierphysiologisches Auslandspraktikum in Australien
2010 - 2011	Diplomarbeit „Kardiale Zell-Zell-Kontakte: Molekulargenetische Untersuchung von Patienten mit genetisch bedingter Herzerkrankung“ im Institut für Rechtsmedizin Frankfurt am Main DNA - Labor, Bereich Forschung
2011 - 2015	Beschäftigung als wissenschaftliche Mitarbeiterin (ab 2013 als Doktorandin der Biologie) im Institut für Rechtsmedizin Frankfurt am Main DNA - Labor, Bereich Forschung

Weiterbildung und Zusatzkenntnisse

- 11. WAVE User Meeting, März 2012, Düsseldorf

- Wiss. Methoden: Phenol-Chloroform-Extraktion,
  Polymerase Chain Reaction (PCR),
  Agarose-Gelelektrophorese,
  Sanger-Sequenzierung,
  Denaturing High-Performance Liquid Chromatography (DHPLC),
  TA-Klonierung, Mutagenese,
  Elektrophysiologie (Patch-clamp mit HEK293-Zellen),
  Confocal Laser Scanning Microscopy (CLSM)

- EDV-Kenntnisse: Word, Excel, Power Point
  Analyseprogramme (SeqScape V2.5, Igor, WCIF ImageJ,
  LAS AF Lite)

- Fremdsprachen: Englisch in Wort und Schrift

Teilnahme an Kongressen und Tagungen

- 8th International Symposium on Advances in Legal Medicine and
  90th Annual Conference of the German Society of Legal Medicine,
  September 2011, Frankfurt am Main

- 91. Jahrestagung der Deutschen Gesellschaft für Rechtsmedizin,
  September 2012, Freiburg (**Vortrag**)

- PhD Course Sudden Cardiac Death, Februar 2013, Kopenhagen, Dänemark

- 92. Jahrestagung der Deutschen Gesellschaft für Rechtsmedizin,
  September 2013, Saarbrücken (**Vortrag**)